

Solar-Powered Rankine Cycle Assisted by an Innovative Calcium Looping Process as an Energy Storage System

*Original*

Solar-Powered Rankine Cycle Assisted by an Innovative Calcium Looping Process as an Energy Storage System / Cannone, S. F.; Stendardo, S.; Lanzini, A.. - In: INDUSTRIAL & ENGINEERING CHEMISTRY RESEARCH. - ISSN 0888-5885. - ELETTRONICO. - 59:15(2020), pp. 6977-6993. [10.1021/acs.iecr.9b05605]

*Availability:*

This version is available at: 11583/2891059 since: 2021-09-23T11:55:58Z

*Publisher:*

American Chemical Society

*Published*

DOI:10.1021/acs.iecr.9b05605

*Terms of use:*

This article is made available under terms and conditions as specified in the corresponding bibliographic description in the repository

*Publisher copyright*

ACS postprint/Author's Accepted Manuscript

This document is the Accepted Manuscript version of a Published Work that appeared in final form in INDUSTRIAL & ENGINEERING CHEMISTRY RESEARCH, copyright © American Chemical Society after peer review and technical editing by the publisher. To access the final edited and published work see <http://dx.doi.org/10.1021/acs.iecr.9b05605>.

(Article begins on next page)

# 1 **Solar-powered Rankine cycle assisted by an innovative** 2 **calcium looping process as energy storage system**

3 *Salvatore F. Cannone<sup>1,2</sup>, Stefano Stendardo<sup>1\*</sup>, Andrea Lanzini<sup>2</sup>*

4 1. ENEA, Italian National Agency for New Technologies, Energy and Sustainable Economic  
5 Development, Casaccia, Roma, Italy

6 2. Energy Department, Politecnico di Torino, Via Duca degli Abruzzi 24, 10129 Torino, Italy

7 \* *Corresponding author: Stefano Stendardo – stefano.stendardo@enea.it*

## 8 **Abstract**

9 Solar energy is an intermittent resource and thus an energy storage system is required for practical  
10 applications of the collected solar irradiance. This work deals with the integration of a thermo-  
11 chemical energy storage (TCES) system based on the Calcium Looping (CaL) process with a  
12 concentrated solar tower power (CSP) plant. The objective of this work is the integration of a  
13 conventional 320 MWe Rankine cycle with a direct calcination for the energy harvesting.  
14 Particularly, this work addresses the use of CO<sub>2</sub> as the working fluid of a compressed-gas energy  
15 storage (CGES) system for hybrid energy storage with CaL process. The hybrid TC/CG-ES  
16 (Thermo-Chemical/Compressed-Gas Energy Storage) system can increase the competitiveness  
17 of the CSP with respect to conventional fossil-based power plants leading to a reduction in CO<sub>2</sub>  
18 emissions. The thermal integration with the Calcium Looping (CaL) system is optimized by  
19 means of the pinch analysis methodology. The obtained results show a reduction in the electrical  
20 efficiency of about four percentage points with respect to the conventional Rankine power cycle  
21 without CSP unit: the net electrical efficiency reduces from 43.7% to 39.5% while the global  
22 (thermal and electrical) efficiency of the plant reaches the peak value of 51.5% when low

23 enthalpy energy is recovered (e.g. district heating network, district cooling network). The paper  
24 highlights the importance of the thermochemical CaO based material. With a conversion of CaO  
25 to CaCO<sub>3</sub> of 80% the storage efficiency defined as the ratio of the energy released during the  
26 carbonation and the CO<sub>2</sub> expansion to the energy collected by the solar field and required during  
27 the CO<sub>2</sub> compression is 87.3%.

## 28 **Keywords**

29 Energy Storage; Calcium Looping; Thermo–Chemical/Compressed–Gas Energy Storage; Use  
30 of compressed CO<sub>2</sub>, Concentrated Solar Power (CSP); Rankine power cycle.

## 31 **Highlights**

- 32 • A novel solar power Rankine cycle with integrated energy storage by calcium looping  
33 process is proposed.
- 34 • Calculated net and global system efficiencies are 39.5% and 51.5% respectively;
- 35 • The electrical efficiency penalty is about 4 percentage points from the conventional  
36 Rankine plant to the solar plant.

## 37 **1 Introduction**

38 Climate change represents a critical issue for our planet and it is time to intensify the efforts of  
39 the researchers and scientists to mitigating the forthcoming impacts. For this purpose, on 12  
40 December 2015, the nations that are members of UNFCCC reached an agreement with the aim  
41 to limit the global warming well below 2.0°C before pre-industrial level and try to reduce it down  
42 to 1.5°C [1]. In order to reach the ‘2°C target’, only 720 Gt of CO<sub>2</sub> can be emitted into the  
43 atmosphere from 2018 to 2100; according to [1] the current rate of CO<sub>2</sub> emission is 32.5 Gt/year.

44 The production of gross electricity has been increasing since 1974, except during economic crisis  
45 that caused a drop in global production. Currently, the largest part of electricity (67.3% of total  
46 electricity production [2] in 2016) is produced with conventional combustion of energy sources  
47 as fossil fuels, biofuel and wastes.

48 At the end of 2023, almost 30% of power demand in the electricity sector will be provided by  
49 renewables reaching also 12.4% of global energy demand [3]. Concentrated solar power will  
50 have the highest growth with respect to the trend of the past five years [3]. New plants will be  
51 constructed in Chile, Morocco and South Africa. However, technology risk, long construction  
52 times and still inefficient energy storage solutions continue to curb the development of this  
53 technology. Generally increasing the variable renewable energy plants there will be same period  
54 during the day in which the energy produced exceeds power demand [4].

55 Concentrated solar power depends on the availability of direct sunlight. Hence, energy storage  
56 systems and more wide flexibility are highly needed [5] to increase the capacity factors of solar-  
57 powered plants and to correct the mismatch between the discontinuous renewable energy supply  
58 and demand. Thus, cheap and efficient energy storage can help to boost the applicability of CSP  
59 and thus contribute to mitigating global warming during the energy transition.

60 Different technologies are used to store energy from CSP plants:

61 - Sensible thermal energy storage systems (STES): The quantity of stored energy  $Q_{sensible}$  is a  
62 function of temperature difference ( $T_h - T_c$ ), specific heat capacity ( $c_p$ ) and mass of stored material.  
63 High specific heat capacity materials are used such as molten salts [6] (nitrates, carbonates,  
64 chlorides) and solids (ceramic materials or graphite).

$$65 \quad Q_{sensible} = m \int_{T_c}^{T_h} c_p(T) dT \quad (\text{Eq.}) 1$$

66 - Phase-change materials (PCM): The quantity of energy stored is highly dependent on the  
67 enthalpy of fusion ( $\Delta h_{fusion}$ ) and the mass of material. The energy can be stored also in sensible

68 form. Latent energy storage materials (inorganic salts, metallic) which can be coupled with  
69 system at very high temperature can have a phase change temperature between 579°C  
70 (Aluminium alloys) and 842°C (Fluorides salts) [7].

$$71 \quad Q_{latent} = m \int_{T_c}^{T_h} c_p(T) dT + m \Delta h_{fusion} |_{T=T_{melting}} \quad (\text{Eq.}) 2$$

72 - Thermochemical energy storage (TCES): solar energy is converted into separately chemical  
73 materials through an endothermic reaction [8]. The stored energy  $Q_{thermochemical}$  is a function  
74 of the enthalpy of reaction  $\Delta h_{reaction}$ , the mass of stored material and sensible heat.

$$75 \quad Q_{thermochemical} = m \int_{T_c}^{T_R} c_p(T) dT + m \Delta h_{reaction} |_{T=T_R} + m \int_{T_R}^{T_h} c_p(T) dT \quad (\text{Eq.}) 3$$

76 Both sensible and latent heat storage systems have a low efficiency due to energy losses in the  
77 short-medium term, instead TCES storage avoids the loss of heat producing stable chemical  
78 compounds that can be stored at ambient temperature. During cloudy days or, generally,  
79 whenever energy is needed, the produced chemical materials are brought together under  
80 favourable thermodynamic conditions in order to promote an exothermic reaction. The released  
81 heat during the reaction can be used to produce electricity and to power a district heating network.

82 Thermochemical storage systems have several advantages :(i) The energy density is about two  
83 to five times higher than PCM and STES systems. A conventional STES, consisting of two tanks  
84 of molten salt based on nitrate (60%  $\text{NaNO}_3$  - 40%  $\text{KNO}_3$ ) with the approximate hot and cold  
85 temperatures between 565°C and 290°C has a storage capacity of 0.731 GJ/m<sup>3</sup> [9]. Latent energy  
86 storage have the advantages to provide heat at constant temperature, the carbonate salts (e.g.  
87  $\text{Li}_2\text{CO}_3$ ) have a high fusion temperature 726°C with a storage density of 1.34 GJ/m<sup>3</sup> [7]. Instead,  
88 this work proposes a thermochemical storage based on calcium looping process, with a reaction  
89 temperature of 895 °C and the energy storage density can reach 3.2 GJ/m<sup>3</sup> [10]; (ii) Since there  
90 is negligible thermal loss during storage via CaL, this technology can be considered as a seasonal

91 storage unlike the others which are used more as daily or weekly storage; (iii) The heat of reaction  
92 is discharged at constant and high temperature.

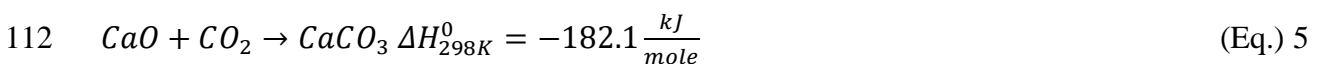
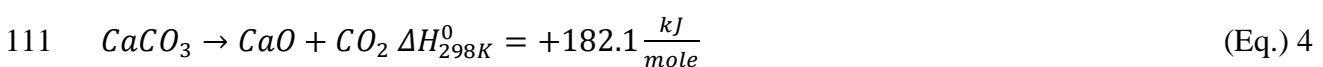
93 The CaL process as energy storage have been proposed in the scientific literature mostly  
94 integrated in a tower solar. In [11] a calciner assisted by CSP to capture CO<sub>2</sub> from flue gas into  
95 carbonator reactor was proposed whereas in [12] [13] [14] the authors have conducted a  
96 comparison between closed and open CO<sub>2</sub> based Brayton cycles with a conventional reheat  
97 Rankine cycle each of the three cycles equipped with a CaL energy storage system fitted with an  
98 indirect calcination reaction. Considering 10% of thermal dispersion in carbonator reactor,  
99  $\Delta T_{\min}=10^{\circ}\text{C}$ , 1% pressure drop in each heat exchange and  $X=0.5$  (average CO<sub>2</sub> conversion) they  
100 have obtained: (i) 35.5% with reheat Rankine cycle; (ii) around 32% with sCO<sub>2</sub> Brayton cycle;  
101 (iii) 39% with a combined cycle that use the integration of CaL process with CO<sub>2</sub> Brayton and  
102 conventional Rankine cycles. However, direct expansion of CO<sub>2</sub> at the exit of the carbonator  
103 reactor is not recommended because it may contain solid particles that would damage the blades  
104 of the turbines placed downstream.

105 The novelty of this paper is the integration of a conventional reheat Rankine cycle assisted by a  
106 CaL system with a direct calcination reaction.

## 107 **2 Calcium Looping as energy storage system**

### 108 **2.1 Fundamentals of Calcium Looping process**

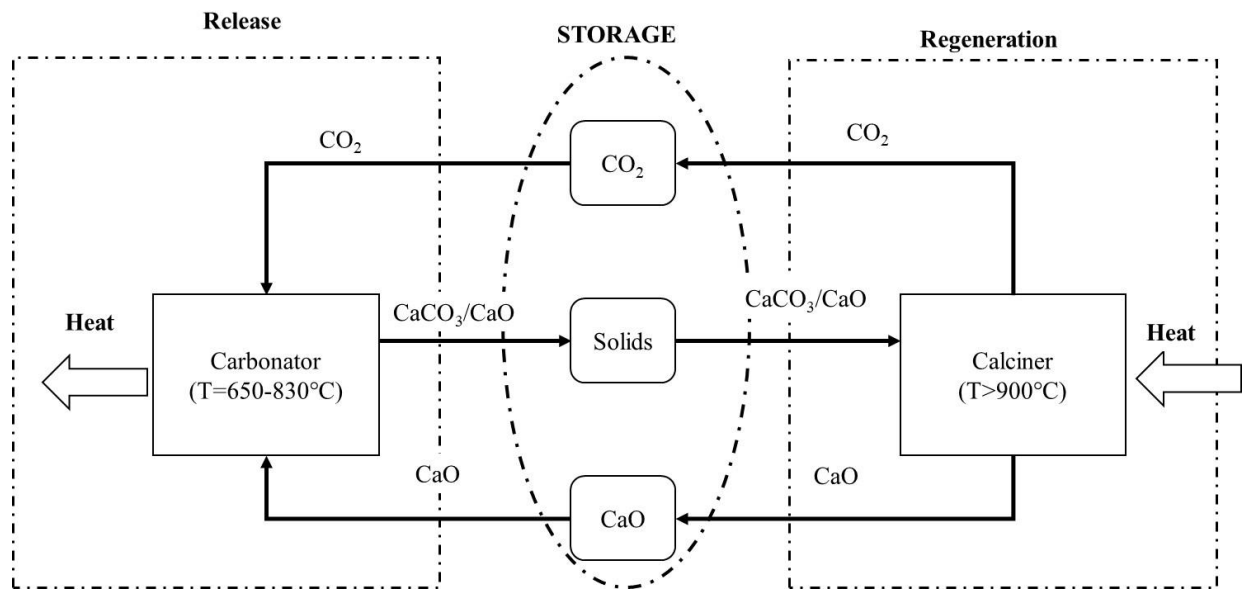
109 Calcium Looping (CaL) is a cyclic chemical process that comprises two key reactions: (i)  
110 calcination of CaCO<sub>3</sub> as reported in Eq. 4 and (ii) carbonation of CaO as reported in Eq. 5.



113 The main advantages of the CaL process is the low market price (9 €/ton [13]) of the CO<sub>2</sub> acceptor  
114 material and the absence of negative impacts for the environment and the health of human beings:  
115 CaO from naturally occurring materials (e.g. limestone or dolomite) are widely available and  
116 harmless towards the environment with several outlet market for spent materials (iron, steel and  
117 cement industries). For instance, commercial limestone rock generally contains more than 90%  
118 of calcium carbonate.

119 Shimitzu et al. [15] proposed for the first time the reaction of CaO with CO<sub>2</sub>, i.e., the calcium  
120 looping process CaL, with the main goal of decarbonizing flue gas. Since the calcination reaction  
121 is endothermic, the heat of reaction is usually supplied by oxy-fuel combustion into the reactor.  
122 CaL process is gaining considerable interest as thermochemical energy storage process where  
123 calcination (Eq.4a) is the process for energy gathering and carbonation (Eq.4b) is the step for  
124 energy release. The carbonator reactor operates in a temperature range between 600 – 850°C with  
125 an operating pressure ranging from 1 bar to 3 bar when outgoing gas is not expanded in a gas  
126 turbine [13]. Since the carbonation reaction is an exothermic reaction, heat is released and steam  
127 can be produced to generate electricity by a submerged heat exchange in a fluidised bed  
128 carbonator. The produced CaCO<sub>3</sub> can be stored and successively transported to the calciner  
129 reactor to gather the excess of energy. Into the calciner reactor, the equilibrium temperature of  
130 the system CaO-CaCO<sub>3</sub>-CO<sub>2</sub> is approximately 895 °C under atmospheric pressure. Therefore,  
131 the decomposition of CaCO<sub>3</sub> into CaO must take place at temperature above 895°C in case the  
132 molar fraction of CO<sub>2</sub> is 1 and the operating pressure of the calciner is 1 atm.

133 The process is illustrated in Figure 1.



134

135 **Figure 1: The Calcium Looping process used as thermochemical storage system. Calcium oxide and carbon**  
 136 **dioxide react together into the carbonator reactor releasing heat of reaction at high temperature when energy**  
 137 **is necessary. The spent material ( $\text{CaCO}_3$ ) and unreacted  $\text{CaO}$  are, at the first time, stored into a silo. These**  
 138 **materials are transported to the calciner to store excess of energy at high temperature with the inverse**  
 139 **reaction.**

140 It is possible to use the heat released during the carbonation at high temperature ( $650 - 830^{\circ}\text{C}$ )  
 141 in order to produce steam to be expanded in a conventional turbine and generate electricity. Direct  
 142 expansion of  $\text{CO}_2$  at the exit of carbonator and calciner is not recommended because it may  
 143 contain solid particles that would damage the blades of the turbines placed downstream.

144 It is demonstrated from several experimental works that calcite and dolomite can be used as  
 145 sorbent for high temperature  $\text{CO}_2$  capture [16]. However, it is also known that  $\text{CaO}$ -based solid  
 146 sorbent are never fully utilized displaying the existence of maximum degree of carbonation  
 147 conversion [16].

148 Stendardo and Foscolo [16] studied the multi-cycle carbonation/calcination reaction of the  
 149 naturally-occurring dolomite. During different experiments they observed progressively decline  
 150 of  $\text{CaO}$  conversion, which drops from 85% to 65% after only 4 cycles. A good strategy could be  
 151 the replacement of natural dolomite with synthetic  $\text{CaCO}_3$  or doped limestone that maintain a  
 152 high degree of sorbent capture capacity. There are many papers in the literature focused on the  
 153 research of synthetic  $\text{Ca}$ -based sorbents that enhance conversion in a multi cycling experiments

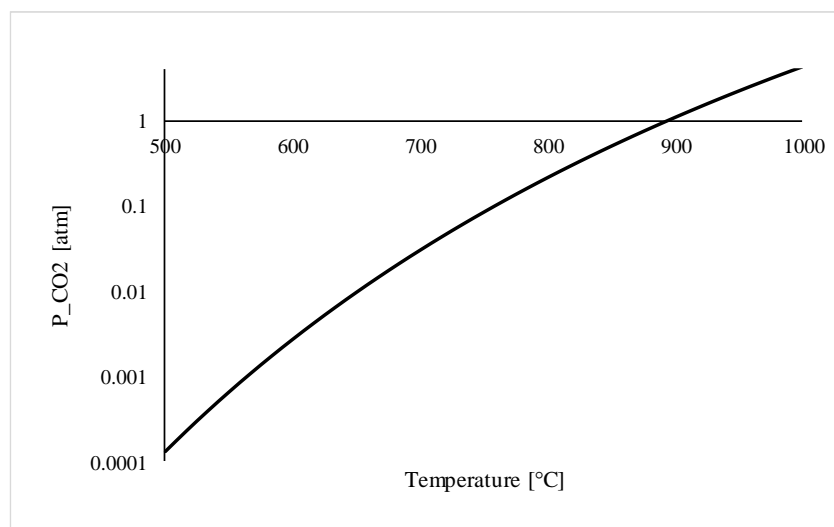
154 [17]. Chen et al. [18] showed that the CO<sub>2</sub> capture capacity of the new materials declines  
155 gradually and at a much slower rate than original limestone during multi-cycle experiments. The  
156 addition of alumina has slowed down the drop in CaO conversion allowing up to 70% percent of  
157 CO<sub>2</sub> capture capacity after 50 cycles.

158 The CO<sub>2</sub>-rich stream leaving the regenerator is cooled, compressed and stored also for long  
159 period (seasonal storage). The produced CaO is cooled and stored in a conventional silo. The two  
160 stored materials are recombined into the carbonator reactor operating at high temperature  
161 (~800°C) to provide heat to a Rankine power cycle. We provide detailed mass and energy  
162 balances of the solar power plant and we calculate the performance of the same plant after energy  
163 integration of various heat sinks/sources of the overall process. This work paves the way for  
164 further demonstration of the concept.

## 165 **2.2 *Integration of CaL with Concentrated Solar Plants***

166 The most common energy storage system for CSP applications is based on molten salts. The  
167 main used components are nitrates, chlorides, fluorides and carbonates. The fluoride salts have  
168 high heat storage capacity (2.3 GJ/m<sup>3</sup>). However, they are very expensive and toxic [19];  
169 chlorides have a high heat of fusion and are very cheap but highly corrosive [20]; carbonates  
170 have high temperature of phase change but high viscosity and they easy decay [21]; nitrate salts  
171 have low chemical reactivity, low corrosiveness and have low cost [7] and therefore suitable for  
172 thermal storage material in CSP. The issues of all the above-described materials are two: (i) the  
173 low melting point limits the efficiency of the system, in fact when the solar energy is not directly  
174 collected, the temperature of the storage has to be higher than melting temperature for each salt  
175 and therefore storage have to be heated; (ii) the low maximum temperature achievable that limits  
176 the (thermal) integration between the CSP field with the thermal storage system and the power  
177 cycle to temperature around 500-600 °C. This limitation is due to degradation of molten salts at  
178 high temperature. The coupling of CSP with CaL process avoids this problem enabling operating

179 temperatures higher than 700°C in carbonator reactor reducing the size of heat exchanger due to  
180 higher temperature difference (maximum temperature of the Rankine heat transfer fluid equal to  
181 538°C). According to thermodynamic equilibrium and kinetics, high temperature is necessary to  
182 drive the calcination reaction when operating under high CO<sub>2</sub> concentrations (~900°C at 1 atm)  
183 [22]. Nevertheless, the use of superheated steam or easily separable gas in calcination  
184 environment decrease the CO<sub>2</sub> partial pressure and therefore, the calcination temperature goes  
185 down to 700-750 °C as shown in **Figure 2** :



186

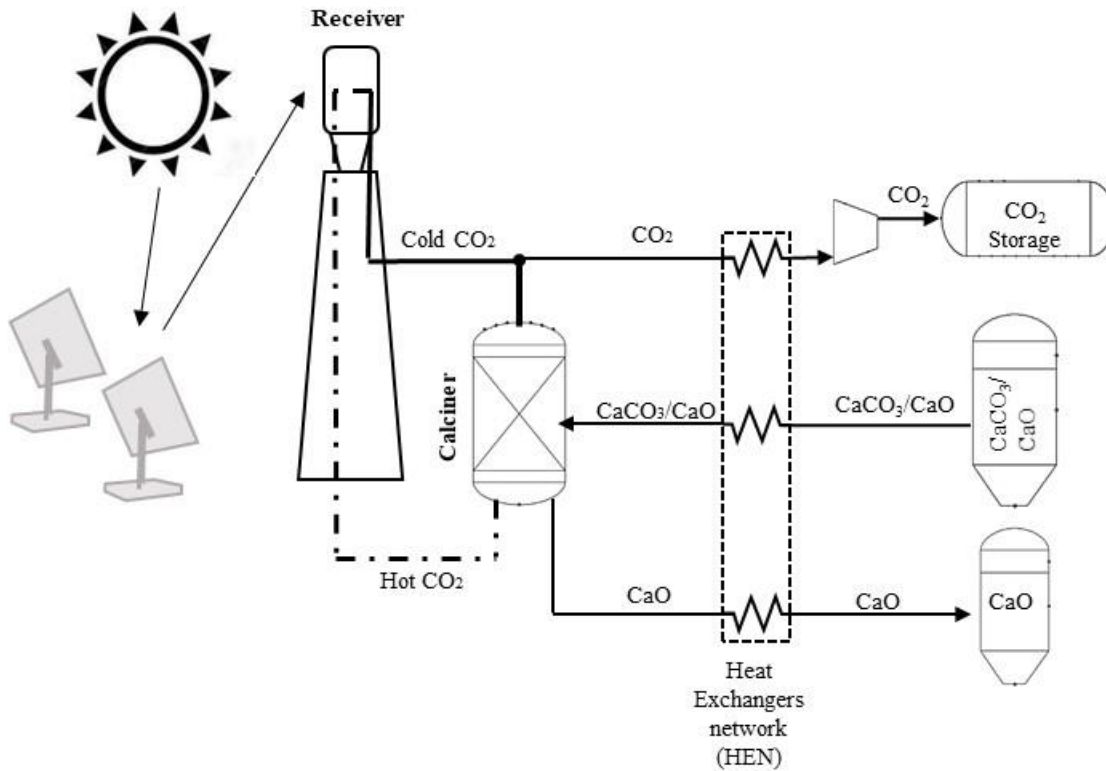
187 **Figure 2: Decomposition pressure of Carbon dioxide over calcium carbonate at different operating**  
188 **temperature [22]**

189 The solutions for solar energy storage via CaL technology can be classified according to the  
190 media used to gather and store the energy. These options are currently classified into (i) indirect  
191 (or mediated) and (ii) direct storage solutions.

### 192 2.2.1 Indirect energy storage

193 In the indirect energy solution, the solar energy is gathered and transferred to a second medium  
194 (Ca-based materials) for its storage. Generally, the gathering medium is a fluid (heat transfer  
195 medium, HTF) whereas the storage medium consists of either liquid or solid materials. Several  
196 configurations have been proposed to harvest solar radiation. Therefore, several prototypes of  
197 solar receiver have been developed as rotary kilns, cyclone atmospheric reactor, falling particle

198 receiver and fluidised bed reactor. As shown in Figure 3 , solar energy is collected into a central  
 199 tower receiver and transferred to a calciner by HTF, which fluidises the  $\text{CaCO}_3/\text{CaO}$  particles. In  
 200 order to not dilute the  $\text{CO}_2$  leaving the calciner, the selected HTF is a pure  $\text{CO}_2$  stream.

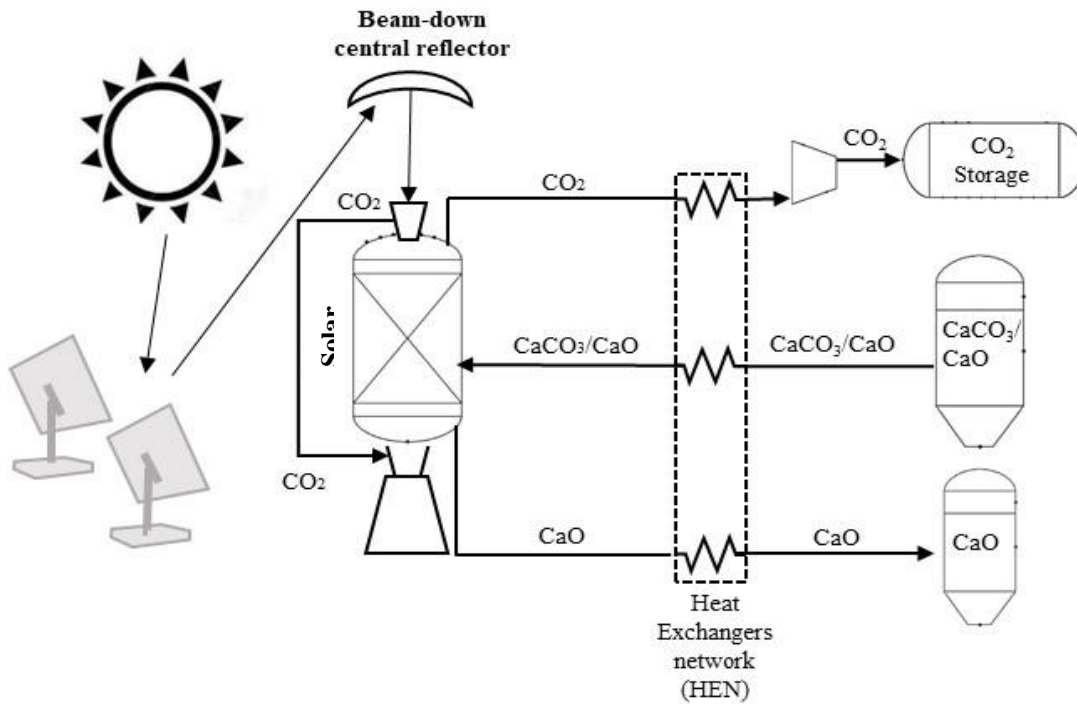


201  
 202 **Figure 3: Integrated Solar Calcium Looping IS-CaL with indirect calcination reaction. Solar energy is**  
 203 **concentrated into a solar receiver up to the tower. The HTF used into this system is the  $\text{CO}_2$  which has the**  
 204 **task to provide the heat necessary for the regeneration of the spent sorbent and to fluidize the calciner.**

205 2.2.2 Direct energy storage

206 In the direct energy storage solutions, the media ( $\text{Ca}$ -based material and  $\text{CO}_2$ ) used for storing  
 207 the energy are as the same as the materials to collect the solar energy into the innovative solar  
 208 calciner reactor. An example of this solution is the gathering of the solar energy and its storage  
 209 via a solid particles fluidised bed [23]. The solar energy reflected by the heliostats are  
 210 concentrated in a single point of the reactor by means of a beam-down central reflector (see  
 211 Figure 4). Therefore, it is possible to have a reactor at a lower height than the classic solar towers,  
 212 reducing the problems of mechanical strength of the structure. Despite the optical losses due to  
 213 another reflector, thermal losses are strongly reduced and therefore higher temperature can be

214 reached [23] [24] [25] [26]. In order to not dilute the CO<sub>2</sub> to store, the fluidised bed will be  
215 fluidised with a recirculation of high-concentrated CO<sub>2</sub> stream.



216

217 **Figure 4: Integrated Solar Calcium Looping IS-CaL with direct calcination reaction into solar calciner. Solar**  
218 **calciner is a solid particles fluidised bed reactor with CO<sub>2</sub> to separate easily the product of calcination**  
219 **reaction. The compounds are stored at ambient temperature to avoid thermal losses.**

220 In this work, a direct solution based on a solid particles fluidised bed solar calciner has been  
221 analysed and investigated Figure 4. The energy is stored in form of chemical compounds (CaO  
222 and CO<sub>2</sub>) that, before reaching the storage tanks, are cooled down by passing through heat-  
223 recovery heat exchangers heating up the calcium carbonate.

224 Solids entering the solar calciner, that are CaCO<sub>3</sub> and unreacted CaO, are pre-heated through a  
225 heat-exchanger network (HEN) by the hot products (i.e. CaO, CO<sub>2</sub>) leaving the calciner. The  
226 solar calciner includes several cyclones and other components that are able to separate the  
227 fluidising CO<sub>2</sub> and product CO<sub>2</sub> from the particles.

228 The excess of solar energy stored in the form of chemical products can be used to generate heat  
229 and electricity with zero CO<sub>2</sub> emissions, solving the problem of dispatchment and intermittency  
230 of renewable energy.

231 The remainder of the work is focused on the analysis of a Rankine cycle assisted by a CaL unit  
232 and powered by a direct solar calcination.

### 233 **3 Rankine cycle assisted by CaL process**

#### 234 **3.1 Description of the Thermo–Chemical/Compressed–Gas Energy Storage**

235 This work analyses a solar powered Rankine cycle assisted by a CaL process as a direct energy  
236 storage solution capable of generating electricity and providing energy to a district heating and  
237 cooling network. The proposed system layout as formulated in Figure 5 can operate in three  
238 different main configurations. The solar energy is collected from the field of heliostats and is  
239 reflected by the beam down central reflector to the solar calciner. The collected energy can be (i)  
240 used directly to generate electricity and/or (ii) stored through direct CaL process.

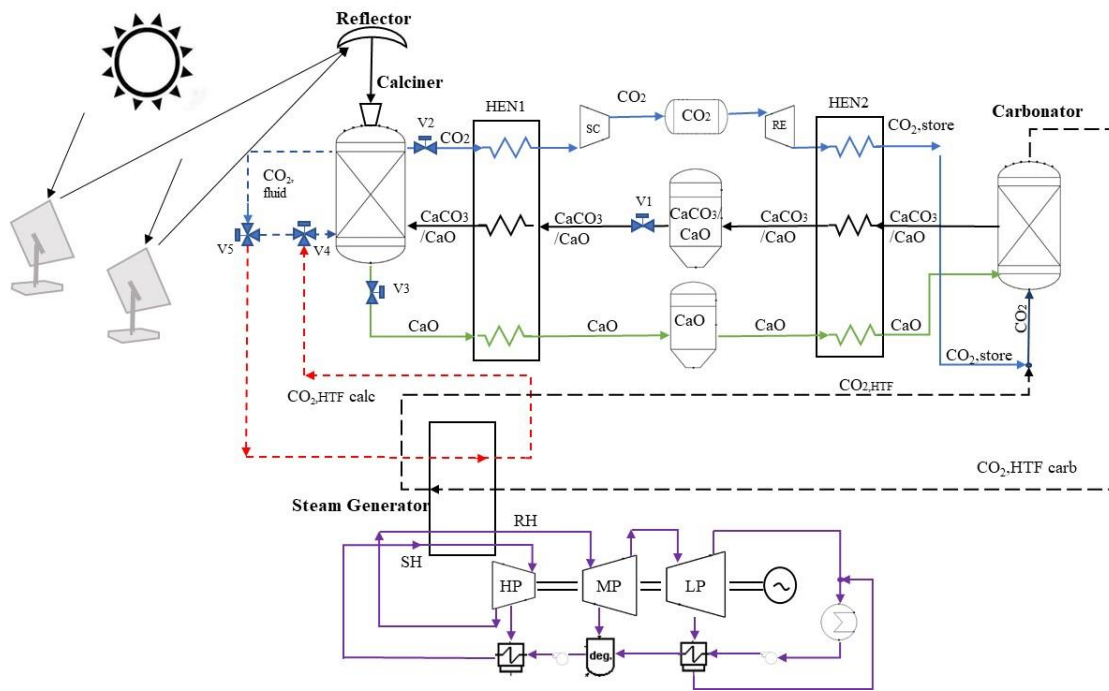
##### 241 **3.1.1 Energy storage**

242 Energy storage takes place in the calciner in which decomposition of CaCO<sub>3</sub> into CaO and CO<sub>2</sub>  
243 occurs at high temperature (900 °C) by means of solar energy input. The solar calciner is a  
244 fluidised bed where the fluidising agent is a pure stream (i.e., CO<sub>2, fluid</sub>) and the solid bed is mainly  
245 composed of CaCO<sub>3</sub> and CaO. The two products of calcination reaction (CO<sub>2</sub> and CaO) are  
246 cooled and stored at ambient temperature to avoid heat losses. Solids entering in the solar  
247 calciner, which consist of CaCO<sub>3</sub> and unreacted CaO, are pre-heated via a heat-exchanger  
248 network (HEN1) by the hot products (i.e. CaO, CO<sub>2</sub>) leaving the reactor. CO<sub>2</sub> stream is cooled,  
249 compressed via the storing compressor (SC) at supercritical conditions and directed to a storage  
250 tank. The cooled CaO stream is transported to a conventional storage site (e.g. silos). Details of  
251 the SC component are provided in section 2.2. Part of the excess of solar heat can be used directly

252 to produce steam via the stream  $\text{CO}_{2, \text{HTF calc}}$ . This option has not been taken into consideration in  
253 the remainder of the paper.

### 254 3.1.2 Energy release

255 During steady state operation, a hot stream (i.e.  $\text{CO}_{2, \text{HTF, carb}}$ ) leaves the carbonator, as shown in  
256 Figure 5, to generate steam in boiler to be used as a working fluid in a Rankine cycle. The heat  
257 required to produce the hot stream  $\text{CO}_{2, \text{HTF, carb}}$  is released by the reaction between CaO and  $\text{CO}_2$   
258 inside the carbonator. Indeed, this reactor is fed by a CaO stream leaving the silos and a  $\text{CO}_2$   
259 stream composed of: (i) a stream leaving the steam generator (i.e.  $\text{CO}_{2, \text{HTF, carb}}$ ) and (ii) a stream  
260 leaving the storage site (i.e.  $\text{CO}_{2, \text{store}}$ ) via a recovery expander (RE). These two components will  
261 be mixed and react releasing the heat and producing the aforementioned hot stream (i.e.  $\text{CO}_{2, \text{HTF, carb}}$ )  
262 leaving the carbonator and making continuous the generation of steam. The storage sites (i.e.  
263 CaO silo and  $\text{CO}_2$  tank) have been sized in order to keep power production continuous (see later  
264 for the details). CaO and  $\text{CO}_2$  entering carbonator are pre-heated via a heat-exchanger network  
265 (HEN2) by the hot product ( $\text{CaCO}_3$ ) leaving the reactor.  $\text{CaCO}_3$  is cooled and stored in  
266 conventional silos. Details of RE component will be given in section 3.2. Figure 5 shows the  
267 Thermo-Chemical/Compressed-Gas Energy Storage (TC/CG-ES) that comprises of: (i) calciner,  
268 storing compressor (SC), (ii) turbo expander (RE) for recovery of energy and (iii) carbonator. In  
269 this mechanical and chemical system, the  $\text{CO}_2$  is used both as working and reacting fluid: it is  
270 compressed in SC and expanded in RE for storing and releasing the energy.

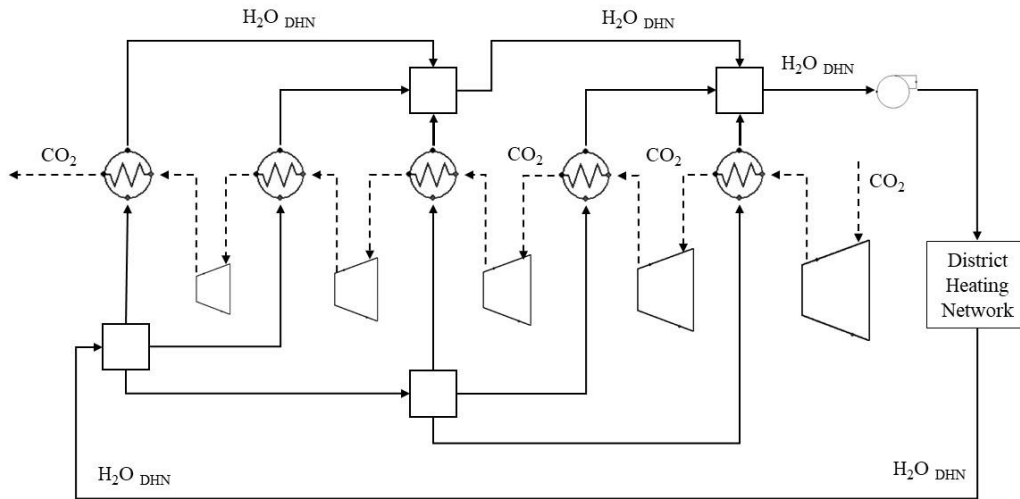


271

272 **Figure 5: Thermo-Chemical/Compressed-Gas Energy Storage (TC/CG-ES) coupled with a conventional**  
 273 **Rankine power cycle. During sunlight solar energy can be transformed directly in electricity or stored in**  
 274 **chemical compound. There are three operational phase: (i) Only electricity is produced; (ii) only charging of**  
 275 **storage system; (iii) Both electricity and chemical compounds are produced.**

276 **3.2 Heat recovery for the CO<sub>2</sub> storage site**

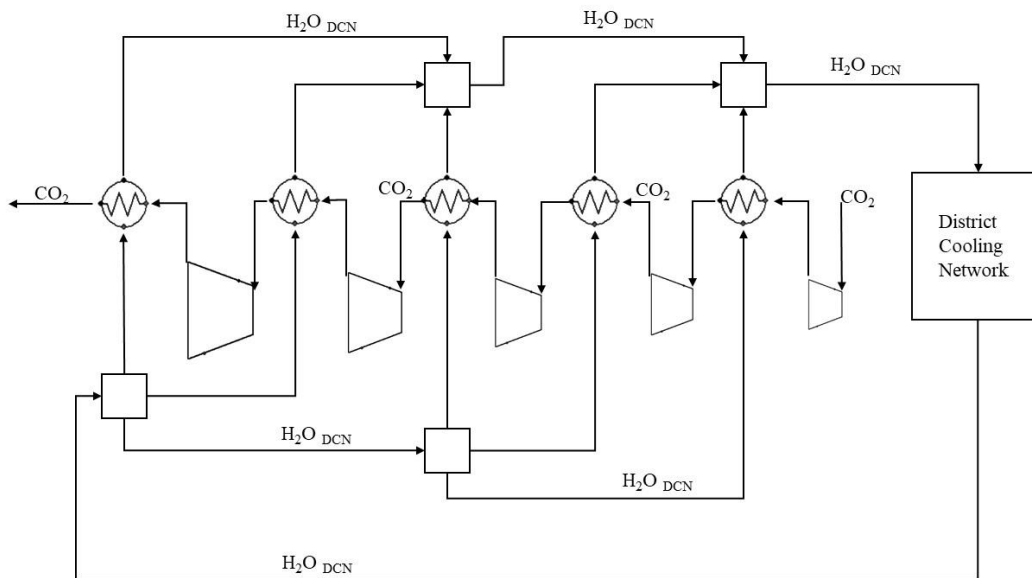
277 The CO<sub>2</sub> is stored at 75 bar by a group of five compressors as shown in Figure 6. The CO<sub>2</sub> is  
 278 stored at supercritical condition to reduce the storage volume [13]. Each compressor has a  
 279 pressure ratio of 2.37 and an isentropic efficiency of 0.83. Each compressor is followed by an  
 280 intercooler to minimize the compression work. The heat collected by the cooling system of the  
 281 compression is used to feed a district heating network. Inside each individual intercooler water  
 282 enters at 60°C and exits at 90°C at a pressure of 4 bar. Subsequently it is pumped up to 10.3 bar  
 283 and sent to the district heating network as is common to do [27].



284

285 **Figure 6: Train of five compressors with five inter-coolers. The heat at low temperature provided during**  
 286 **compression, supply a district heating network.**

287 From the storage unit (see Figure 5), the CO<sub>2</sub> stream feeds the carbonator reactor to react with  
 288 calcium oxide. The expansion of previously stored CO<sub>2</sub> supplies useful work and provide  
 289 efficiently cooling power. The expansion from 75 to 2 bar requires the use of inter-heating  
 290 expansion to avoid the condensation of CO<sub>2</sub> and protect the turbine blades as showed in Figure  
 291 7. This Cooling system provides water at 6 °C and the same return into inter-heating at 12 °C.



292

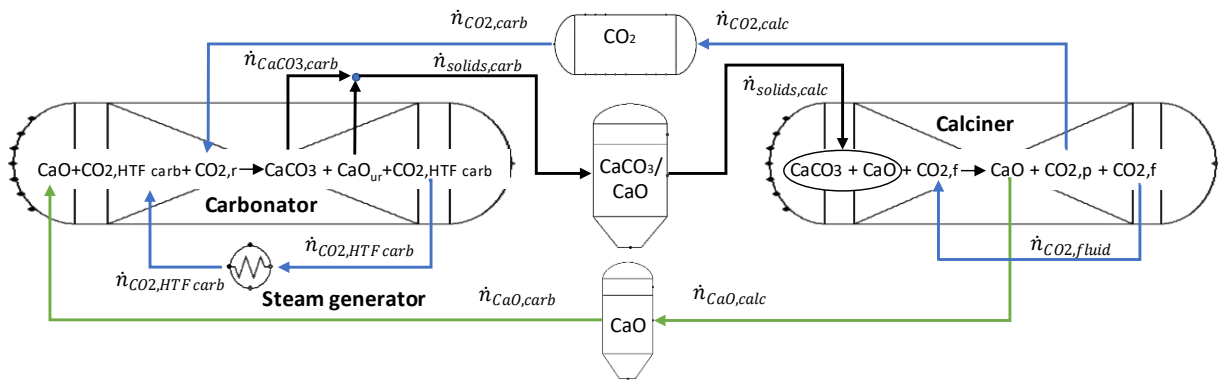
293 **Figure 7: District cooling network used to avoid the condensation of the CO<sub>2</sub> and associate danger for the blade of turbine.**  
 294 **The water used into the inter-heating at 12°C, is cooled until 6°C.**

295 During heat release, CO<sub>2</sub> previously expanded, CaO from reservoir and the CO<sub>2</sub> used as heat  
 296 transfer fluid are heated and then come into carbonator reactor where the release of energy occurs  
 297 (see Figure 5). Under favourable conditions in the carbonator (P= 2bar; T= 850°C), CO<sub>2</sub> and part  
 298 of CaO react in an exothermic reaction and the heat produced at higher temperature is transferred  
 299 at power system throughout the CO<sub>2, HTF</sub>. The solids stream composed of CaCO<sub>3</sub> and un-reacted  
 300 CaO, is cooled and stored inside tank almost at ambient condition.

301 The carbonator reactor is connected to power cycles indirectly by CO<sub>2</sub> which acts both as  
 302 fluidising agent and heat transfer fluid. The CO<sub>2</sub> at high temperature does not produce work  
 303 directly in turbine. Therefore, the pressure of the carbonator reactor is set a 2 bar to overcome  
 304 the pressure drops in the reactor and in the various heat exchangers however, it is not higher than  
 305 2 bar because increasing pressure, the storage efficiency goes down as it is showed in 4.3 section.

### 306 3.3 Energy and mass balance equations

307 The Figure 8 illustrates the molar streams of CaL system equipped with storage.



308  
 309 **Figure 8: Molar balance schematic of the Calcium Looping process. In the right side calcination reaction and energy**  
 310 **storage happen; In the other side CaO and CO<sub>2</sub> react into carbonator reactor and the heat of reaction is transported by**  
 311 **the CO<sub>2</sub> used as HTF.**

312 Into carbonator reactor, a carbonation reaction at 830°C and 2 bar occurs. Here the CO<sub>2</sub> that  
 313 coming out from pressurize storage ( $\dot{n}_{CO_2,r,carb}$ ) react with the CaO ( $\dot{n}_{CaO,carb}$ ). Into the reactor  
 314 the excess of CO<sub>2</sub> which acts as heat transfer fluid ( $\dot{n}_{CO_2,HTF,carb}$ ) flows. Calcium oxide does not  
 315 react completely with the CO<sub>2</sub> due to loss of reactivity during different cycles and depending on

316 the thermodynamic condition and residence time. The flow rate of the unreacted CaO is  $\dot{n}_{CaO\ ur}$ .  
 317 Thus only part of the CaO reacts to produce CaCO<sub>3</sub> ( $\dot{n}_{CaCO_3\ carb}$ ) and therefore solids ( $\dot{n}_{solids\ carb}$ )  
 318 at the carbonator outlet are composed of CaCO<sub>3</sub> and unreacted CaO. Indeed, CaO-based solid  
 319 sorbent are never fully utilized displaying the existence of maximum degree of carbonation  
 320 conversion, nevertheless it is fortunately possible regenerate all the calcium carbonate [16].

$$321 \quad \dot{n}_{CaO\ carb} + \dot{n}_{CO_2\ r,carb} + \dot{n}_{CO_2\ HTF\ carb} \rightarrow \dot{n}_{solids\ carb} + \dot{n}_{CO_2\ HTF\ carb} \quad (\text{Eq.})6$$

$$322 \quad \dot{n}_{solids\ carb} = \dot{n}_{CaCO_3\ carb} + \dot{n}_{CaO\ ur} \quad (\text{Eq.}) 7$$

323 The CaCO<sub>3</sub> phase contained in the solids stream ( $\dot{n}_{solids\ calc}$ ) entering the calciner will be  
 324 completely regenerated to produce calcium oxide ( $\dot{n}_{CaO\ calc}$ ) and carbon dioxide ( $\dot{n}_{CO_2\ calc}$ ) that  
 325 will be compressed and stored.

$$326 \quad \dot{n}_{solids\ calc} + \dot{n}_{CO_2\ HTF\ calc} \rightarrow \dot{n}_{CaO\ calc} + \dot{n}_{CO_2\ calc} + \dot{n}_{CO_2\ HTF\ calc} \quad (\text{Eq.}) 8$$

$$327 \quad \dot{n}_{solids\ calc} = \dot{n}_{CaCO_3\ calc} + \dot{n}_{CaO\ calc} \quad (\text{Eq.}) 9$$

328 One of the most important parameters for this technology is the average CaO conversion (X)  
 329 useful to quantify the amount of CaO converted to CaCO<sub>3</sub> during carbonation reaction. This  
 330 reaction extent is defined as follows:

$$331 \quad X = \frac{\dot{n}_{CaCO_3\ carb}}{\dot{n}_{CaO\ carb}} \quad (\text{Eq.}) 10$$

332 In order to guarantee a steady state condition during the storage and release of energy, the solid  
 333 material regenerated into calciner reactor has to be enough to produce the required heat during  
 334 carbonation. The carbonator has to release the required energy for the whole operational time  
 335 whereas the calciner is able to regenerate the solid material for a shorter time (eight hours  
 336 approximately) when the solar energy is gathered. As a consequence, an adequate storage volume  
 337 is required to store solids (i.e. CaO and CaCO<sub>3</sub>) and CO<sub>2</sub> to continuously feed carbonator during

338 the energy demand. In order to guarantee a steady state condition during power production, the  
 339 sorbent regenerated into calciner reactor has to be enough to produce heat into carbonator side.  
 340 Therefore, the following equation has to be satisfied:

$$341 \int_0^{24} \dot{n}_{CaCO_3 carb}(t) dt = \int_0^8 \dot{n}_{CaO calc}(t) dt \quad (\text{Eq.}) 11$$

342 The left-hand side represent the mole of CaCO<sub>3</sub> producing into the carbonator reactor during the  
 343 24-h time span. This term has to be equal to the mole of CaO regenerated into the calciner. It is  
 344 possible to write  $\dot{n}_{i,in}$  and  $\dot{n}_{i,out}$  the molar rate of the i-th component that comes in and comes out  
 345 respectively from one of two calciner and carbonator reactors.

346 The extent of reaction that represents the degree of reaction (e.g.  $\varepsilon = 1$  the reactants react  
 347 completely) can be defined as:

$$348 \varepsilon = \frac{\dot{n}_{i,out} - \dot{n}_{i,in}}{\nu_i} \quad (\text{Eq.}) 12$$

349 where  $\nu_i$  is the stoichiometric coefficient the molar rate reacted is written as:

$$350 \dot{n}_{i,out} - \dot{n}_{i,in} = \varepsilon \nu_i \quad (\text{Eq.}) 13$$

351 Arranging the first law of thermodynamic and considering that the out flow is at the same  
 352 condition of the reactor, the power heat provided by CSP plant to regenerate completely the  
 353 sorbent is:

$$354 \dot{n}_{CO_2 HTF calc} \cdot [h_{CO_2 HTF}(T_{calc}) - h_{CO_2 HTF}(T_{in})] + \dot{n}_{solids calc} \cdot [h_{solids calc}(T_{calc}) -  
 355 h_{solids calc}(T_{in})] + \varepsilon_{calc} \Delta H_{react}(T_{calc}) = \Phi_{CSP} \quad (\text{Eq.}) 14$$

$$356 \varepsilon_{calc} = \frac{\dot{n}_{CaCO_3 calc out} - \dot{n}_{CaCO_3 calc in}}{\nu_{CaCO_3}} \quad (\text{Eq.}) 15$$

357 The energy balance of the carbonator reactor can be written to compute the molar flow rate of  
 358 the CO<sub>2</sub> needed to remove part of the heat of carbonation reaction:

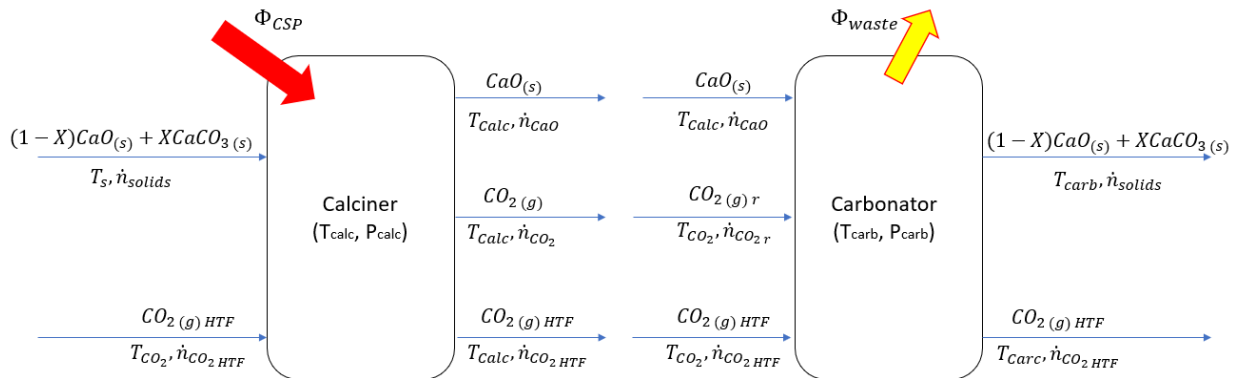
$$\begin{aligned}
359 \quad & (\dot{n}_{CO_2 HTF carb} + \dot{n}_{CO_2 r,carb}) \cdot [h_{CO_2}(T_{carb}) - h_{CO_2}(T_{CO_2 in})] + \dot{n}_{CaO carb} \cdot [h_{CaO carb}(T_{carb}) - \\
360 \quad & h_{CaO carb}(T_{CaO in})] + \varepsilon_{carb} \Delta H_{react}(T_{carb}) = \Phi_{waste} \quad (Eq.) 16
\end{aligned}$$

$$361 \quad \varepsilon_{carb} = \frac{\dot{n}_{CaO carb out} - \dot{n}_{CaO carb in}}{v_{CaO}} \quad (Eq.) 17$$

362 With the heat of reaction defined as:

$$363 \quad \Delta H_{react}(T_{react}) = \Delta H^{\circ}_{react} + \sum_i v_i \cdot \int_{T_{ref}}^{T_{react}} c_{p i}(T) dT \quad (Eq.) 18$$

364 Mass and energy balance are represented in Figure 9.



365

366 **Figure 9: Energy balance of the storage system focused on the main critical reactors.**

#### 367 **4 CaL process integrated with Rankine power cycle**

368 A reheat power Rankine cycle with eight extraction streams with 320 MW groups with 43.7%

369 efficiency is used to produce electricity [28]. Within the power plant, 1023.3 tonne per hour of

370 water circulates, which must be heated by the heat transfer fluid (HTF) leaving the carbonator.

371 Turbine and pump efficiencies values of 83% have been considered as well as a heat exchangers

372 minimum temperature difference of 20°C. On the other hand, non-pressure drops are assumed.

373 All the main operating parameters of the Rankine power cycle are summarised in the following

374 **Table 1.**

375

**Table 1: Main process parameters of the Rankine power cycle [28]**

|                         |        |
|-------------------------|--------|
| $T_{in,HP}$ [°C]        | 538    |
| $P_{in,HP}$ [bar]       | 170    |
| $G_{in,HP}$ [t/h]       | 1023   |
| $T_{in,MP}$ [°C]        | 538    |
| $P_{in,MP}$ [bar]       | 37.7   |
| $G_{in,MP}$ [kg/h]      | 835430 |
| $T_{in,LP}$ [°C]        | 322    |
| $P_{in,LP}$ [bar]       | 7.2    |
| $G_{in,LP}$ [kg/h]      | 738100 |
| $\eta_{is,turbine}$ [-] | 0.83   |
| $\eta_{is,pump}$ [-]    | 0.83   |
| $T_{out,reg}$ [°C]      | 267    |
| $\Delta T_{min}$ [°C]   | 20     |
| $W_{Rankine}$ [MW]      | 320    |
| $\eta_{Rankine}$ [-]    | 0.437  |

376 The high pressure (HP) turbine of the investigated Rankine cycle plant operates at a pressure of  
 377 170 bar and super-heated and re-super-heated temperature of 538°C.

378 In Italy, these plants represent the baseload for power production). The plants located in the  
 379 internal areas are generally built for operation with oil fuel that with natural gas. Oil is supplied  
 380 by pipelines or by tankers or rail tankers. Natural gas is supplied through methane pipelines.

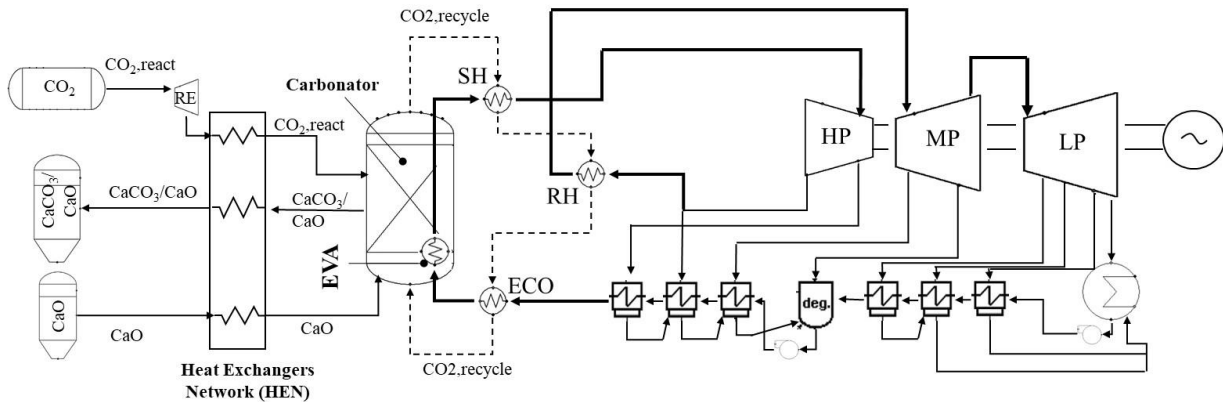
381 The use of the CaL process in a CSP allows storing the excess of renewable energy by producing  
 382 chemical compounds (i.e. CaO and CO<sub>2</sub>). An indirect coupling of CaL to a Rankine cycle for  
 383 generating power was analysed. Thermochemical storage must provide the necessary reagents so  
 384 that the exothermic reaction supplies the heat requirement to the steam.

385 The heat is mainly supplied in four components (see Figure 10)

386 - Water evaporation occurs inside the water-tube walls (EVA) that absorb part of the heat  
 387 of reaction;

388 - At the exit of fluidized bed, the CO<sub>2</sub> used as a heat transfer fluid (HTF) enters the  
 389 superheater (SH) at 830°C, heating the steam at high pressure up to 538°C;

390 - then it enters the re-heater (RH), heating the medium pressure steam (about 37 bar) up to  
 391 538°C;  
 392 - Finally, the CO<sub>2</sub> HTF enters the economizer, heating the liquid water up to 267 °C and  
 393 coming back to the carbonator at 287°C;  
 394 It was analysed the case in which Rankine power cycle was fed only with the carbonator. To  
 395 optimize the heat exchangers network of (HEN), a pinch analysis of the storage system integrated  
 396 with the Rankine cycle is performed.



397  
 398 **Figure 10: Release of energy via TC/CG–ES integrated with Rankine power cycle. The CO<sub>2,recycle</sub> fluidises the**  
 399 **carbonator reactor and transfer heat to Rankine cycle.**

400 **4.1 Optimisation of the heat exchangers network**

401 Pinch analysis is a useful technique to optimise the heat exchanged in energy systems minimising  
 402 external supply of heat and cold. The easiest and often most expensive way is to use external hot  
 403 or cold resources. The most efficient way is to couple the different fluids through heat exchangers  
 404 where simultaneous heating and cooling among the streams happens. To achieve this purpose, it  
 405 is necessary to provide a heat recovery system thus building a network of heat exchangers.  
 406 However, this analysis must always take into account the constraint of the second law of  
 407 thermodynamics, while the difference in temperature between the cold and hot fluids must be  
 408 sufficiently high to not result in excessive heat exchange surfaces.

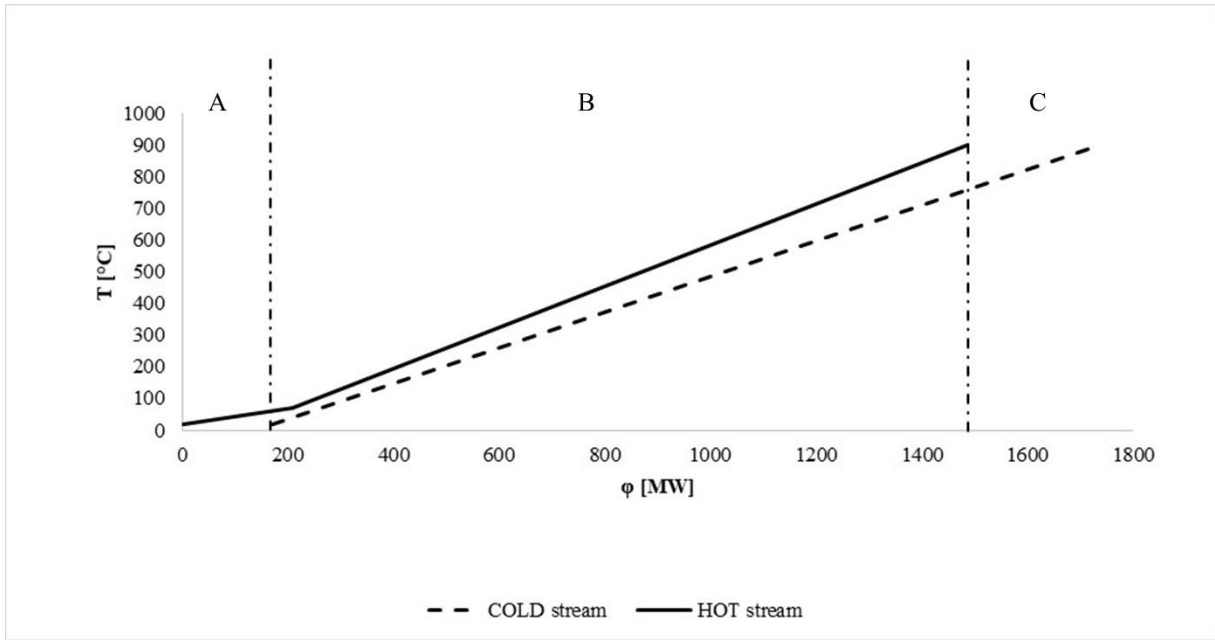
409 The analysis will be carried out separately for the two sides of the storage system (i.e. heat storage  
 410 side and heat release side). The storage area composed of silos and pressurised tank of CO<sub>2</sub> is  
 411 placed in the between of the calciner and carbonator in order to be able to separate not only  
 412 temporally but also physically the storage (calciner) from the release (carbonator) of energy.

413 The first step of the analysis consists in identifying the components of the system and the related  
 414 entering or exiting fluids. The energy storage system is composed of the reactor itself in which  
 415 the calcination reaction occurs and the CO<sub>2</sub> compression system. The latter consists of five  
 416 compressors with the relative inter-cooling system that exchanges heat with water acting as heat  
 417 transfer fluid in the district heating network. The CO<sub>2</sub> compression system is reported as SC in  
 418 Figure 5 and Figure 12.

419 **Table 2: Streams identified during the pinch analysis of the calciner side**

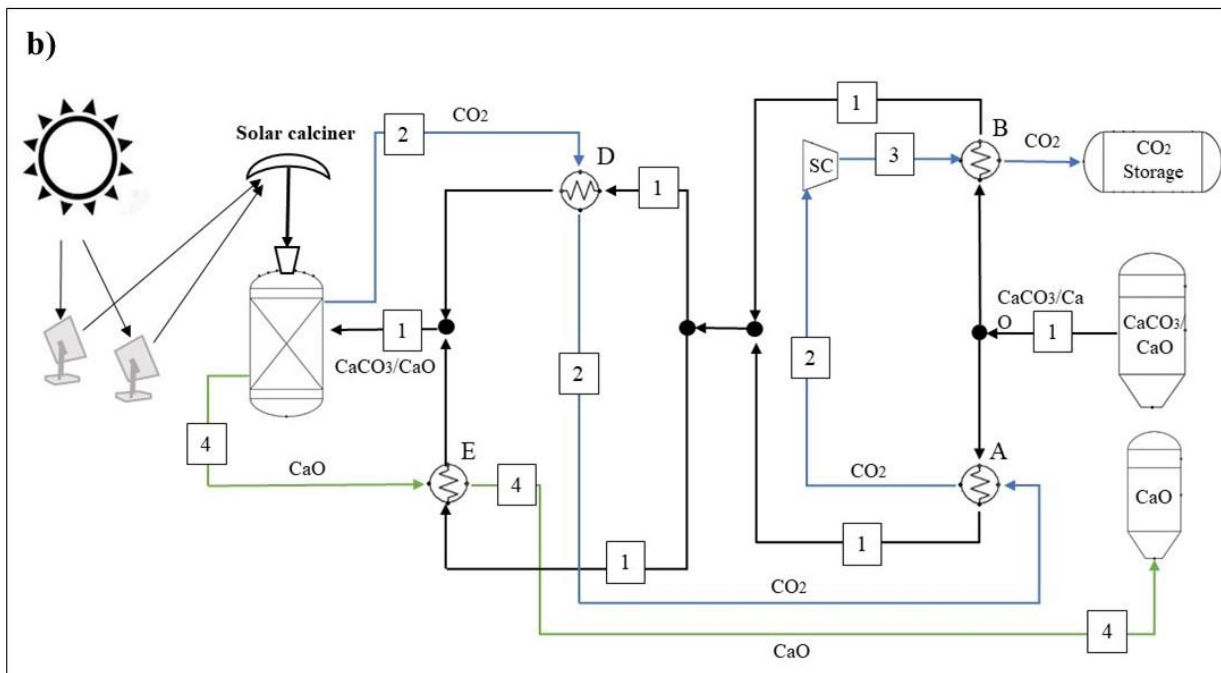
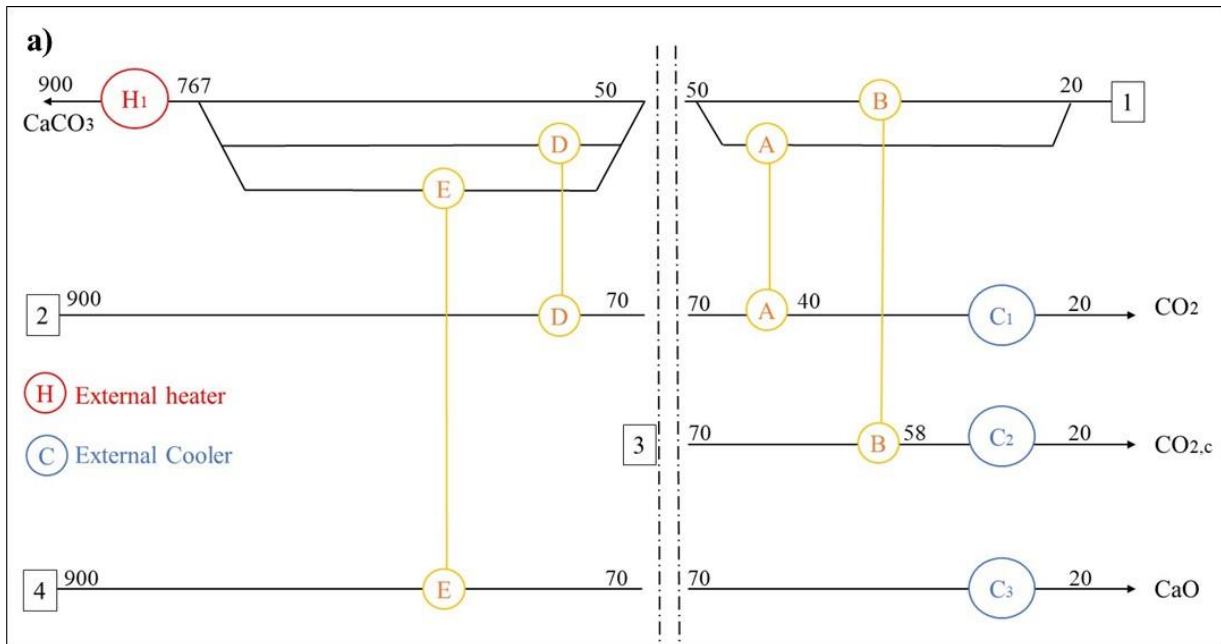
| # of stream<br>pynch | Component       | Type of<br>stream | T <sub>in</sub><br>[°C] | T <sub>out</sub><br>[°C] | Mass rate<br>[kg/s] | G x cp<br>[MW/K] | Power Heat [MW] |
|----------------------|-----------------|-------------------|-------------------------|--------------------------|---------------------|------------------|-----------------|
| 1                    | Solids          | COLD              | 20                      | 900                      | 1540,4              | 1,78             | -1566,5         |
| 2                    | CO <sub>2</sub> | HOT               | 900                     | 20                       | 594,13              | 0,66             | 582,4           |
| 3                    | CO <sub>2</sub> | HOT               | 70                      | 20                       | 594,13              | 2,67             | 133,4           |
| 4                    | CaO             | HOT               | 900                     | 20                       | 946,3               | 0,88             | 770,6           |

420  
 421 Four fluid streams are identified (see **Table 2**), three of which are hot streams (i.e. (2) CO<sub>2</sub> leaving  
 422 the calciner; (3) CO<sub>2</sub> leaving the compressor; (4) CaO leaving the calciner) and one cold stream  
 423 (solids stream entering the calciner). The only cold fluid is made up of solids (i.e. X CaCO<sub>3</sub> and  
 424 (1-X) CaO) that will be sent to the calciner in which a full regeneration of the sorbent takes place.  
 425 A fixed value of CaO conversion to CaCO<sub>3</sub> (X=0.7) has been used.



426

427 **Figure 11: Composite curve of the solar calciner side. Section A represents the excess of heat at low**  
 428 **temperature; in section B the hot streams provide heat to cold streams; in section C there aren't hot streams**  
 429 **and the heat enough is provided by CSP to cold streams**



430  
 431 **Figure 12: a) Minimum energy consumption network inferred from the pinch analysis in the calciner side.**  
 432 **The values of temperature level are reported in degree Celsius. b) Plant configuration (calciner-side) resulting**  
 433 **from the pinch analysis**

434 The result of the pinch analysis is the HEN showed in Figure 12. As you can see, in this case  
 435 incoming stream ( $\text{CaCO}_3$ ) into calciner reached a temperature of  $767^\circ\text{C}$  due to the HEN. The  
 436 remaining sensible energy to heat the spent solids up to  $900^\circ\text{C}$  is provided by the heat exchanger  
 437 H1 (238 MW) which represents part of the energy gathered by CSP (2432 MW). The remaining  
 438 energy necessary to drive the calcination and decompose  $\text{CaCO}_3$  into the respective CaO and

439 CO<sub>2</sub> will be provided also by the CSP (2194 MW). The configuration of HEN, the phase change  
 440 fluids and chemical reaction were treated following the methodology described in [29].

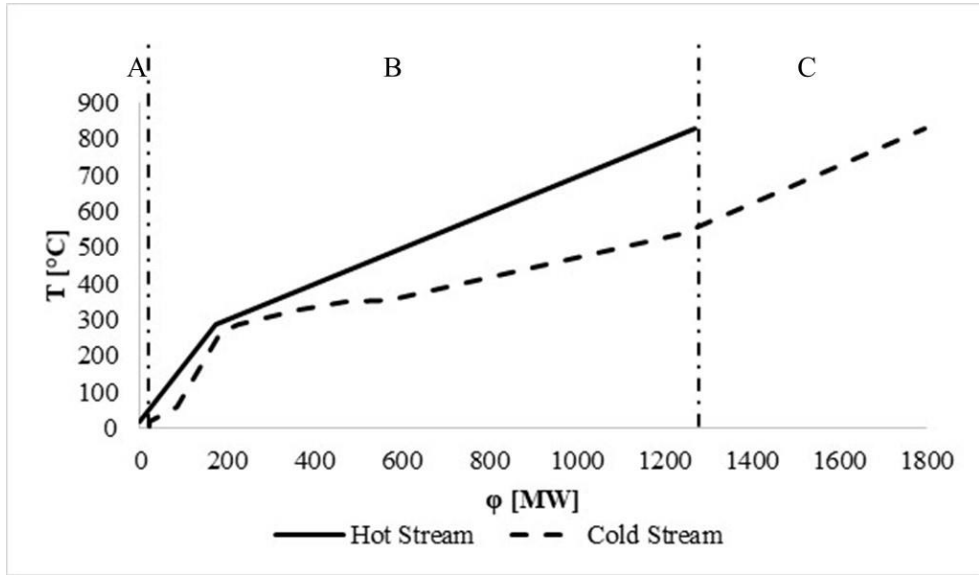
441 Following the analysis thoroughly performed for the energy storage, the pinch analysis for the  
 442 carbonator section was also performed (energy release). The energy release section is mainly  
 443 composed of two devices: (i) the carbonator in which the carbonation reaction occurs, and (ii)  
 444 the turbine train in which compressed CO<sub>2</sub> is expanded from 75 to 2 bar. Through the expansion  
 445 of CO<sub>2</sub> in the RE component (see Figure 5), it is possible to produce both power and cooling.  
 446 After each expansion stage, the carbon dioxide is at the temperature of about -30 ° C and must  
 447 be heated in order to avoid condensation and the consequent breakage of the blades. The heat  
 448 released by the water in a refrigerant cycle (see Figure 7) is transferred to the CO<sub>2</sub> which is heated  
 449 from -30 °C to 7 °C. The refrigerant fluid is sent to a second heat exchanger where it is heated  
 450 up and an external environment is cooled (e.g. hospital). The size of the power chiller is  
 451 approximately 29 MW. Table 3 shows that the pinch analysis which accounts for ten fluids, two  
 452 of which are hot streams leaving the carbonator at a temperature of 830 ° C and the remaining  
 453 are cold streams to be heated as reported in Figure 14.

454 **Table 3: Streams identified during the pinch analysis of the carbonator side**

| # of stream pynch | Component | Type of stream | T_in [°C] | T_out [°C] | Mass rate [kg/s] | G x cp [MW/K] | Power Heat [MW] |
|-------------------|-----------|----------------|-----------|------------|------------------|---------------|-----------------|
| 1                 | CO2       | HOT            | 830       | 287        | 1173,6           | 1,3721        | 745,1           |
| 2                 | Solids    | HOT            | 830       | 20         | 513,48           | 0,6489        | 525,6           |
| 3                 | H2O(l)    | COLD           | 267       | 352        | 284,25           | 1,6263        | -138,24         |
| 4                 | H2O       | COLD           | 352       | 353        | 284,25           | 97,7600       | -97,76          |
| 5                 | H2O(v)    | COLD           | 353       | 538        | 284,25           | 1,2078        | -223,45         |
| 6                 | H2O(v)    | COLD           | 325,9     | 538        | 232,064          | 0,5402        | -114,57         |
| 7                 | CO2       | COLD           | 20        | 60         | 198,045          | 1,0353        | -41,41          |
| 8                 | CO2       | COLD           | 7         | 287        | 198,045          | 0,1900        | -53,20          |
| 9                 | CO2       | COLD           | 287       | 830        | 1371,645         | 1,6035        | -870,68         |
| 10                | CaO       | COLD           | 20        | 830        | 315,43           | 0,2908        | -235,55         |

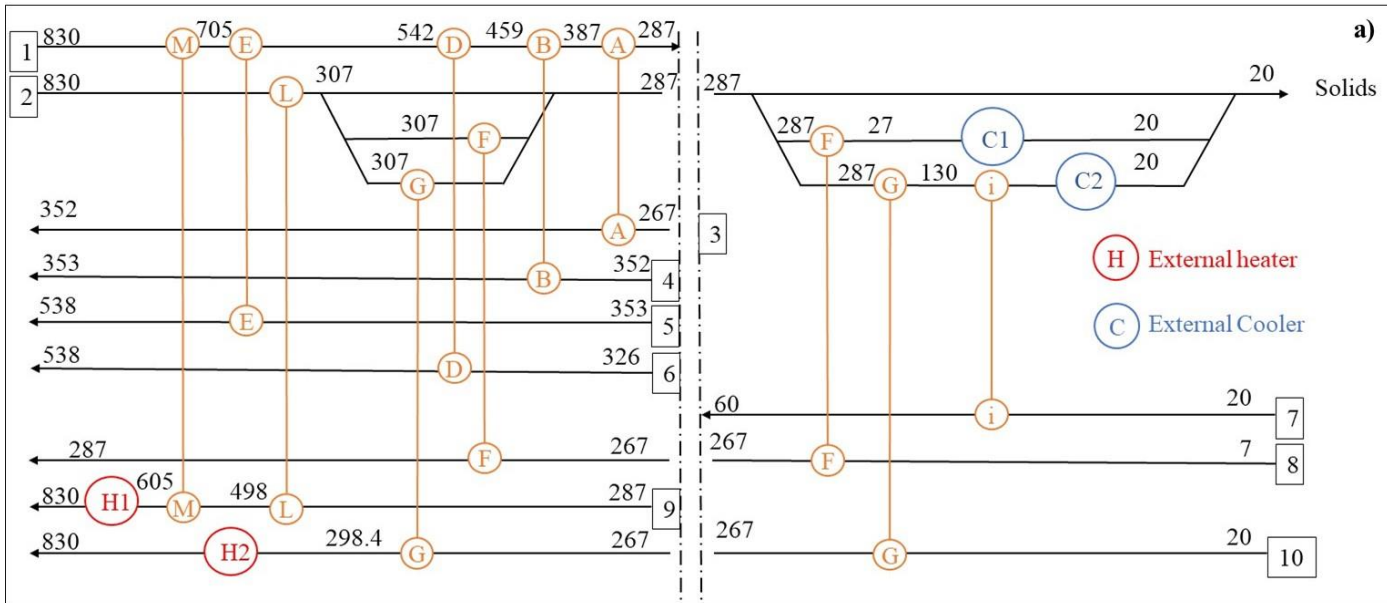
455 The cold fluids are (see *Figure 14*): (7) the compressed CO<sub>2</sub>, which is heated before entering the  
 456 turbine in order to produce more power, (8) the CO<sub>2</sub> at the end of expansion, which temperature

457 between 7 ° C to 287 ° C (minimum temperature of recirculation CO<sub>2</sub>), (9) the CO<sub>2</sub> entering the  
 458 reactor ranging from 287 ° C to the carbonation temperature, (10) CaO heated from ambient  
 459 temperature to carbonation temperature, and finally (3-6) the working fluid of a conventional  
 460 Rankine cycle, which is subjected to preheating, evaporation, overheating and re-heating.



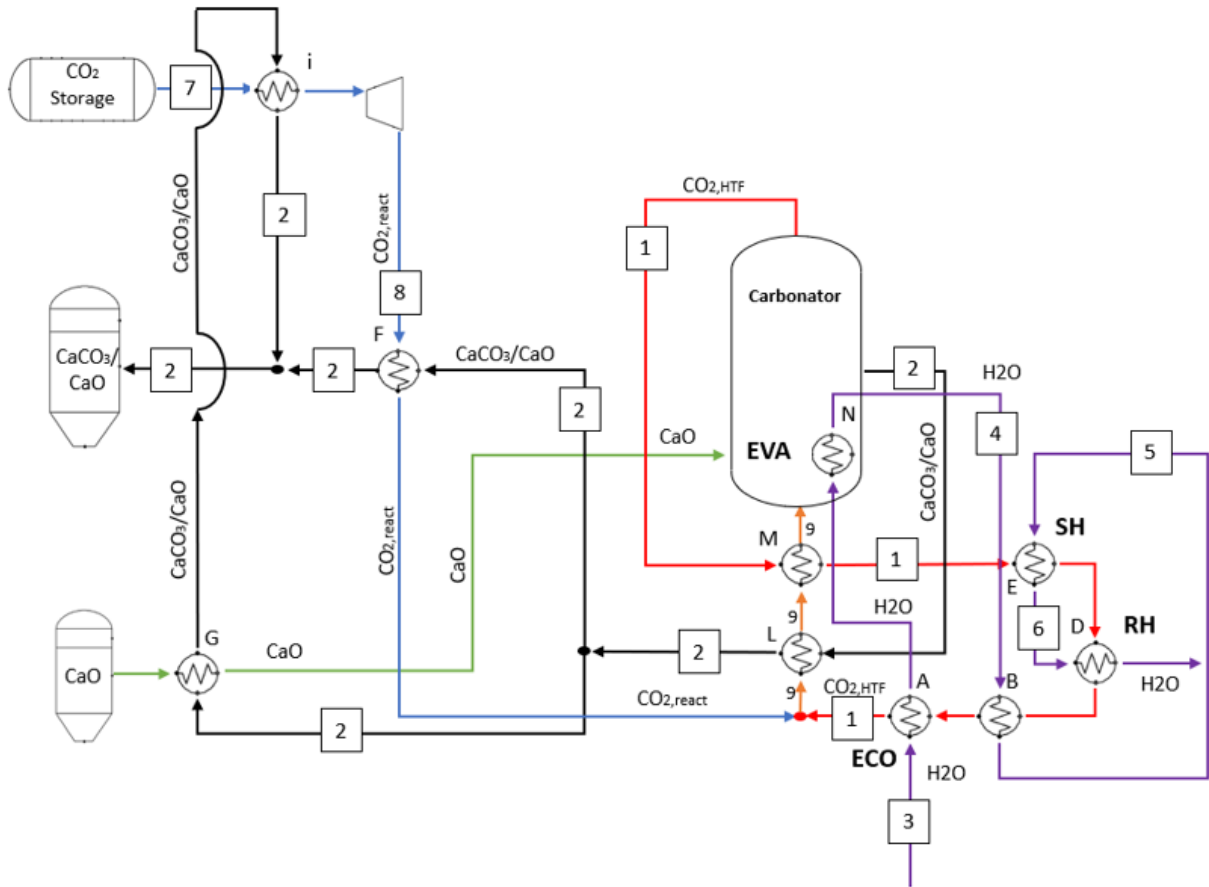
461

462 **Figure 13: Composite curve of the carbonator side. Section A represents the excess of heat at low temperature;**  
 463 **in section B the hot streams provide heat to cold streams; in section C there aren't hot streams and the heat**  
 464 **enough is provided by carbonation reaction to cold streams**



465

b)



466

467 **Figure 14: a) Minimum energy consumption network inferred from the pinch analysis in the calciner side.**  
 468 **The values of temperature level are reported in degree Celsius. b) Plant configuration (carbonator-side)**  
 469 **resulting from the pinch analysis.**

470 The final goal of the analysis is to select a HEN which can be used in parametric analysis with  
 471 regards to key operating parameters (e.g. X, operating temperature and pressure). In *Figure 14.b*  
 472 is showed the final HEN through pinch analysis to carbonator section. At the exit of economizer,  
 473 saturate water flows into water-tube wall (exchanger N) and a partial evaporation (title of vapour:  
 474 0.635) occurs due to heat released by carbonation reaction (165MW). This fluid is not represented  
 475 in pinch analysis because it cannot be coupled with other. The remaining heat of evaporation is  
 476 provided by hot CO<sub>2</sub> (1). The heat of exothermic carbonation reaction heats fluids 9-10 (569MW)  
 477 until temperature of reaction. The overall heat of carbonation reaction is 745 MW. 569 MW is  
 478 used to pre heat the reactants and HTF. Almost the 4% of 172.2MW is lost to the environment.  
 479 165MW is used to partial evaporation of water in water-tube wall.

## 480 **4.2 Process model description**

481 The commercial software Chemcad<sup>TM</sup> was used for the modelling and simulation of the Rankine  
482 cycle power plant integrated with calcium looping technology. This is used to solve material and  
483 energy balances of complex systems providing a large database of chemical components. It is  
484 designed to simulate chemical reactions with regards to the power production.

485 Both the Rankine cycle plant and the CaL unit were simulated through several components such  
486 as reactors, flow mergers/splitter, heat exchangers. Due to the large amount of sub-processes  
487 taking place and to their complexity, some simplifying assumptions had to be made:

- 488 - Operation of all components is at steady state;
- 489 - Only thermodynamic equilibrium has been considered;
- 490 - The ambient temperature and pressure are constant and equal to 20°C and 1 bar,  
491 respectively;
- 492 - The pressure losses were neglected;
- 493 - The heat losses in the piping and in the rest of the system were neglected with the  
494 exception of the carbonator reactor in which about 4% of heat produced is lost.
- 495 - The performance of the main reactors e.g. carbonator and calciner were represented using  
496 the chemical and phase equilibrium through the free energy minimization at the operating  
497 temperature;
- 498 - A complete calcination of calcium carbonate takes place into solar calciner;
- 499 - Minimum temperature difference (pinch temperature) is 20°C for all main heat  
500 exchangers and 10°C for intercooler;

501 - The plant is equipped with a solid-solid heat exchanger, gas-solid heat exchanger and  
502 with gas-gas regenerator.

503 Several of this assumption are summarized in the **Table 4**.

504 **Table 4: Main operating data of the Calcium Looping storage system**

|                                               |         |
|-----------------------------------------------|---------|
| Solar heat provided to calciner [ $MW_{th}$ ] | 2431.58 |
| Thermal dispersion in carbonator [%]          | 3.85    |
| Calciner temperature [ $^{\circ}C$ ]          | 900     |
| Calciner pressure [bar]                       | 1       |
| Ambient temperature [ $^{\circ}C$ ]           | 20      |
| CaO average conversion [%]                    | 70      |
| Carbonator Temperature [ $^{\circ}C$ ]        | 830     |
| Carbonator Pressure [bar]                     | 2       |
| CO <sub>2</sub> storage conditions [bar]      | 75      |
| Daylight hours [h]                            | 8       |
| Isentropic efficiency [%]                     | 83      |

505  
506 The thermodynamic equilibrium is supposed to be reached in both carbonator and calciner  
507 reactors: the molar flow of calcium oxide feeding the carbonator was set to react with the CO<sub>2</sub>  
508 flowing through the RE providing the heat enough to run the Rankine cycle. According to  
509 experimental results [18] an average CaO conversion X of 0.7 was selected.

510 The thermal energy input required by the calciner is mainly due to the decomposition of calcium  
511 carbonate to calcium oxide and carbon dioxide. Consequently, the calciner energy consumption  
512 is estimated based on the average amount of solids sent into the regeneration/storage step.

513 In addition, a complete conversion of CaCO<sub>3</sub> to CaO into the calciner operating at 900 $^{\circ}C$  has  
514 been supposed. The performance of the calciner as well as the carbonator were analysed using  
515 the Gibbs free energy minimization model.

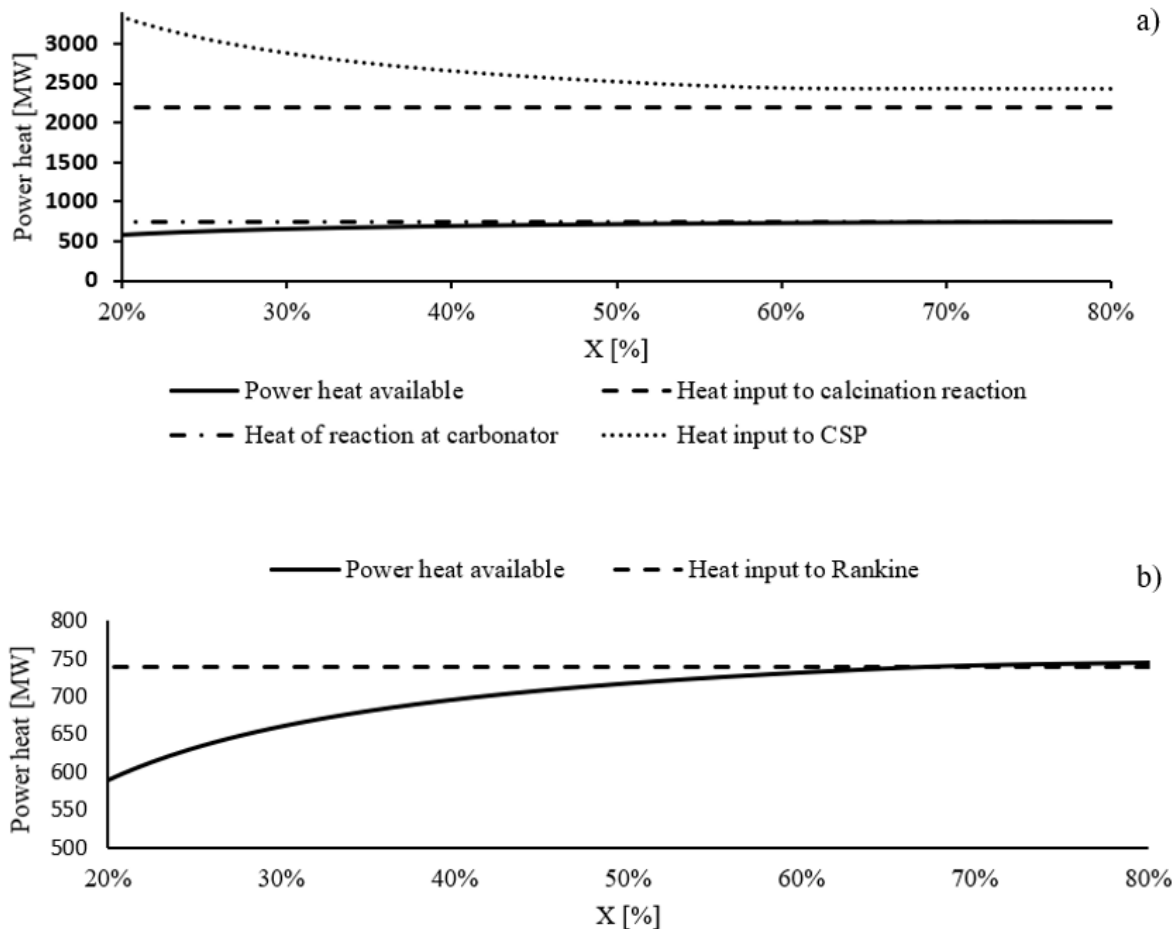
516 The CaL process requires a continuous make-up flow of fresh limestone to counteract the  
517 deactivation of lime with the number of carbonation/calcination cycles while a corresponding

518 purge is also extracted from the calciner. The calcined purge is a potential material to be fed to  
519 the cement plant and other industrial process (e.g. iron and steel, glass and pulp). Due to the high  
520 resistance of the new sorbents at higher number of cycles and the negligible fine production, a  
521 continuous make-up flow is not simulated.

### 522 **4.3 Parametric analysis and process simulation results**

523 In order to evaluate how the performance of the sorbent affects the previously selected HEN, a  
524 parametric analysis was carried out by varying the CaO conversion  $X$ . This parameter has an  
525 important influence on the system as whole: in particular, for the selection of (i) size of storage  
526 vessels, (ii) solids flow rates and (iii) heat requirements.

527 As mentioned above, we are considering the case in which: (i) the electric power is produced  
528 through the heat transferred only by the carbonator to the Rankine cycle and (ii) the CSP is used  
529 only to regenerate the spent sorbent. The heat transferred from CSP to the Rankine cycle is  
530 negligible compared to the heat transferred by the carbonator to the Rankine cycle. The thermal  
531 energy produced by carbonator reactor has to meet the Rankine cycle and heat the inert materials  
532 entering with the active CaO. During this analysis, the power production of the Rankine cycle is  
533 fixed. **Figure 15** shows the effect of the CaO conversion on the thermal power in both main  
534 reactors in which the carbonation and calcination reaction occur.



535

536 **Figure 15: a) Thermal power fluxes of main reactors at varying CaO conversion. b) The heat enough from**  
 537 **Rankine cycle is fixed, while change the heat provides by the storage system.**

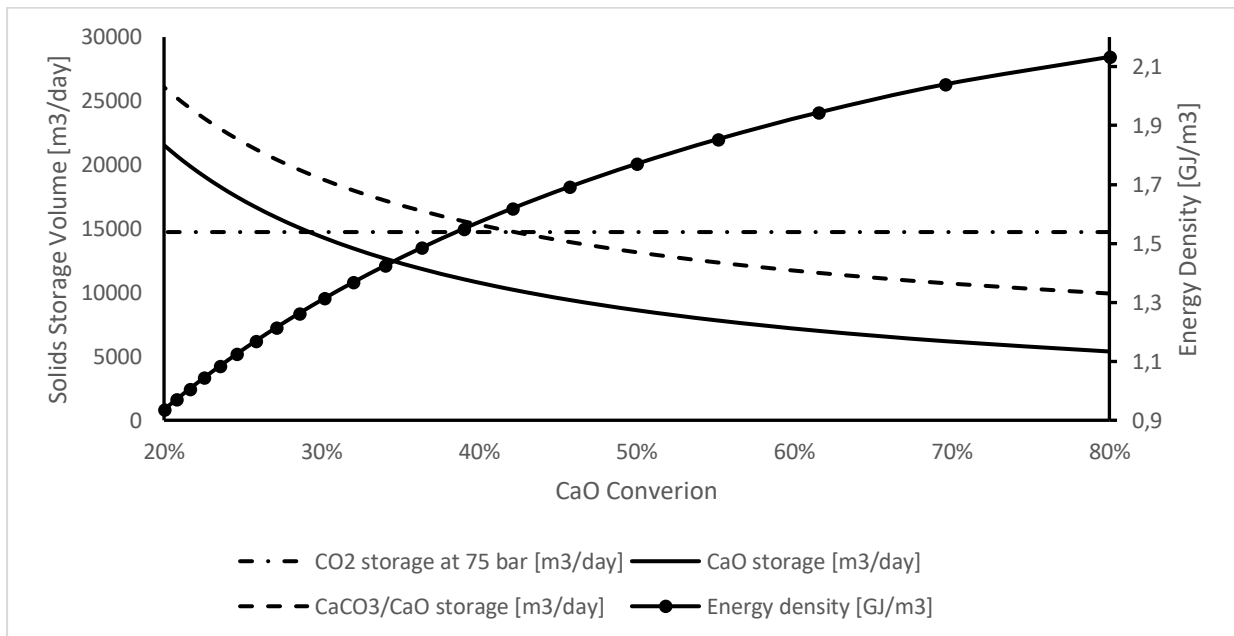
538 By fixing the quantities of the compounds that must react in the reactors (4.5 kmol/s both CO<sub>2</sub>  
 539 and CaO), the necessary thermal power, produced respectively in the calciner ( $\Phi_{\text{calc}} = -2194$  MW)  
 540 and carbonator ( $\Phi_{\text{carb}} = 745$  MW) reactors due to reactions, remain constant. The sensible heat  
 541 necessary to heat up the reactants to the temperature of the respective reactor, decreases  
 542 significantly at high CaO conversion. This means that the lower the conversion of the CaO, the  
 543 higher the molar flow rate of the solids and therefore the energy needed to heat up the entering  
 544 solids increases.

545 Therefore, in case of loss of performance of the sorbent (low X), it may be necessary:

546 • Reduce the power produced, thus producing less energy in the carbonator;

- 547 • Use an external resource that provides the remaining power;
- 548 • Increase the flow rate of the reagents (CaO and CO<sub>2</sub>), making the system operating at
- 549 nominal power with less hours per day;

550 **Figure 16** shows that increasing the CaO conversion, storage volume of the solid streams decreases  
 551 while the CO<sub>2</sub> storage is not affected. This last observation is due to the fact that the CO<sub>2</sub> required  
 552 for the carbonation reaction has not changed. The CO<sub>2</sub> storage volume is strongly depending on  
 553 the thermodynamic storage conditions.



554 **Figure 16: Parametric analysis: Daily storage volume with the change of CaO conversion**

555 Another important parameter to evaluate and compare energy storage system is the energy  
 556 density, represented in the same figure at different values of CaO conversion. It is illustrated that  
 557 with small values of CaO conversion, the solids storage volume increase and therefore the energy  
 558 density goes down starting from 2.1 MJ/m<sup>3</sup> to 0.95 MJ/m<sup>3</sup>.

560 A key performance indicator (KPI) to evaluate thermal efficiency during one cycle of  
 561 carbonation/calcination is the *Thermal Storage efficiency*. It is calculated considering only the  
 562 thermal energy released to carbonation reaction and the energy input to calciner reactor over 24h.

$$\eta_{TSE} = \frac{Q_{carbonator}}{Q_{CSP}} \quad (\text{Eq.}) 19$$

Thermal storage efficiency takes into account the only thermal energy of the storage avoiding the summing of thermal power and mechanical power used in the next KPI and it is useful to compare other energy storage.

However, it is relevant also the storage condition and not only output/input thermal energy. The KPI to evaluate the effectiveness of the storage and release system is the *storage efficiency*, defined as the ratio of the heat released during carbonation reaction plus expansion work of CO<sub>2</sub> to the heat gathered by the CSP plus the compression work required during CO<sub>2</sub> storage.

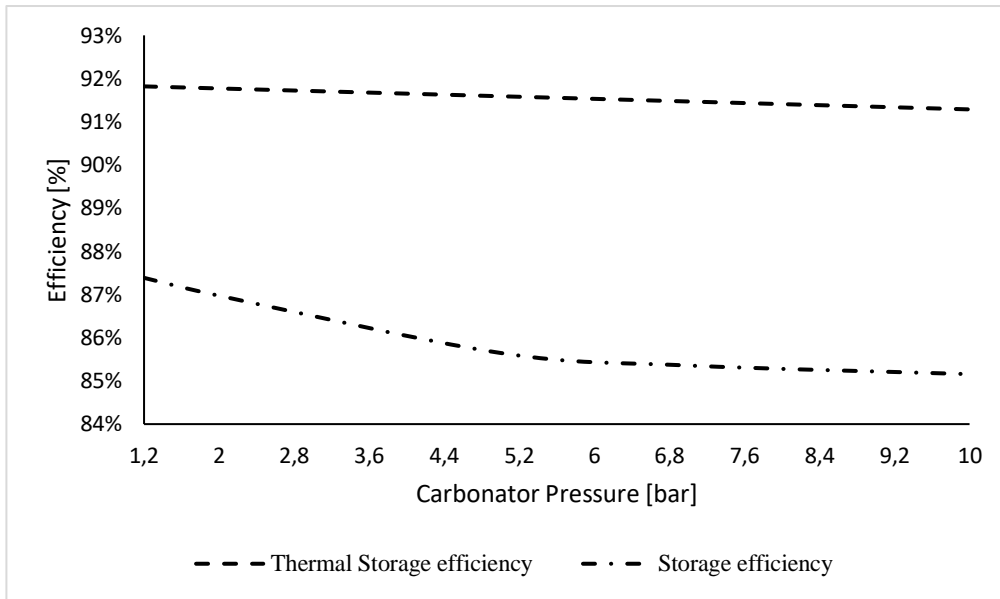
$$\eta_{SE} = \frac{Q_{carbonator} + L_{CO_2, expansion}}{Q_{CSP} + L_{CO_2, compression}} \quad (\text{Eq.}) 20$$

In order to take in consideration other benign effects of the system the following *storage and recovery efficiency* has been formulated: This parameter takes into account the low enthalpy heats exchanged by the storage system through the system boundary to the district heating and cooling network.

$$\eta_{SRE} = \frac{Q_{carbonator} + L_{CO_2 expansion} + Q_{district cooling} + Q_{district heating}}{Q_{CSP} + L_{CO_2 compression} + L_{pump}} \quad (\text{Eq.}) 21$$

Each term of the KPI represents an energy and it is calculated by multiplying the thermal or mechanical power by the respective operating time.

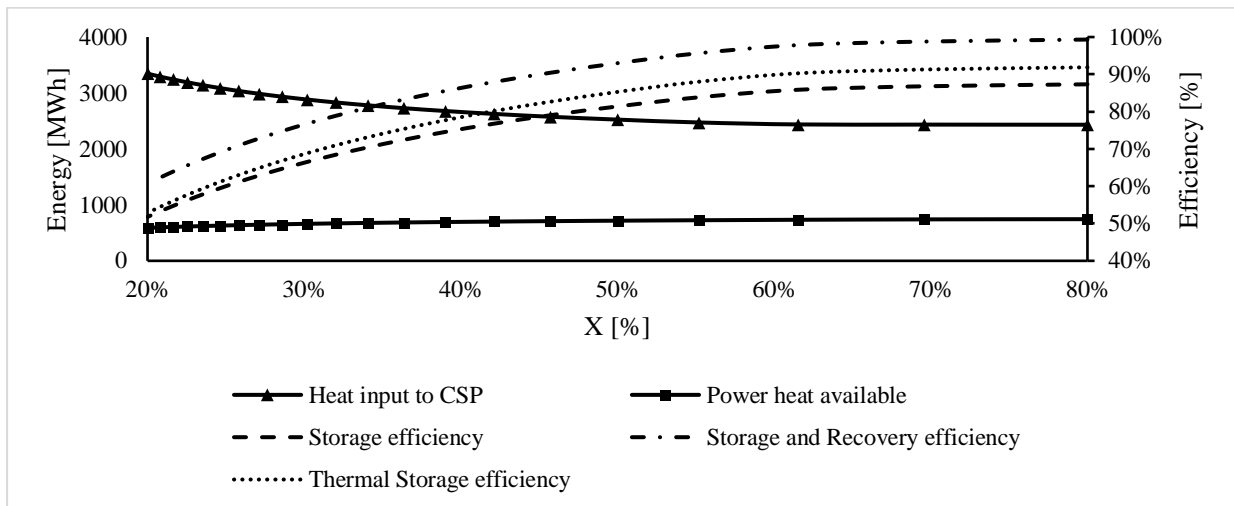
At first time, a parametric analysis to assay the pressure condition of carbonator reactor was performed (**Figure 17**) and it was visible that increasing carbonator pressure, the heat of reaction goes down ( $\eta_{TSE}$ ) while it is highlighted that electric power due to expansion work of CO<sub>2</sub> drop off ( $\eta_{SE}$ ).



583

584 **Figure 17: Trend of two KPI (Thermal Storage efficiency and Storage efficiency) function of carbonator**  
 585 **pressure.**

586 The maximum differences in Thermal Storage efficiency ( $\eta_{TSE}$ ) and Storage efficiency ( $\eta_{SE}$ )  
 587 increasing carbonator pressure are 0.6% and 2.6% respectively. As mentioned in previous  
 588 section, carbonator pressure is set at 2 bar to ensure the circulation of gas in all storage system  
 589 leading a reduction in the efficiencies mentioned above by 0.1% and 0.5% respectively.



590 **Figure 18: It is illustrated with whole line the thermal energy (left axis) of the heat provided by carbonator**  
 591 **reactor (square indicator) and heat input to CSP power plant (triangle indicator). With the dash line is**  
 592 **represented the three different efficiency of the storage system (right axis). These parameters are function of**  
 593 **CaO conversion.**

595 **Figure 18** shows the comparison of the storage efficiency (right axis) with the energy stored and  
 596 released with the change of the CaO conversion X. The efficiency of the storage system increases

597 with high values of released energy and low values of solar energy required. Storage and recovery  
 598 efficiency is always higher than storage efficiency and thermal storage efficiency because it takes  
 599 into account the heat at low enthalpy exchanged with the district heating and cooling network.  
 600 The three KPIs (thermal storage efficiency, storage efficiency, storage and recovery efficiency)  
 601 represented in **Figure 18** increase significantly with the increasing of X and they reach a value of  
 602 91.9%, 87.3% and 99.3% respectively when CaO conversion is higher (X=80%). Therefore, it is  
 603 better to work with a material having excellent conversion performance and recover the energy  
 604 at low temperature to achieve very high levels of efficiency for a storage system.

605 Three other fundamental key performance indicators for the integrated system consider the power  
 606 generated by the Rankine cycle turbines. In this case, the optical and thermodynamic efficiencies  
 607 of the CSP were not considered in this analysis. The three KPIs are below defined:

608 *i. Integrated efficiency*

$$609 \quad \eta_{IE} = \frac{L_{Rankine}}{Q_{CSP}} \quad (\text{Eq.}) \quad 22$$

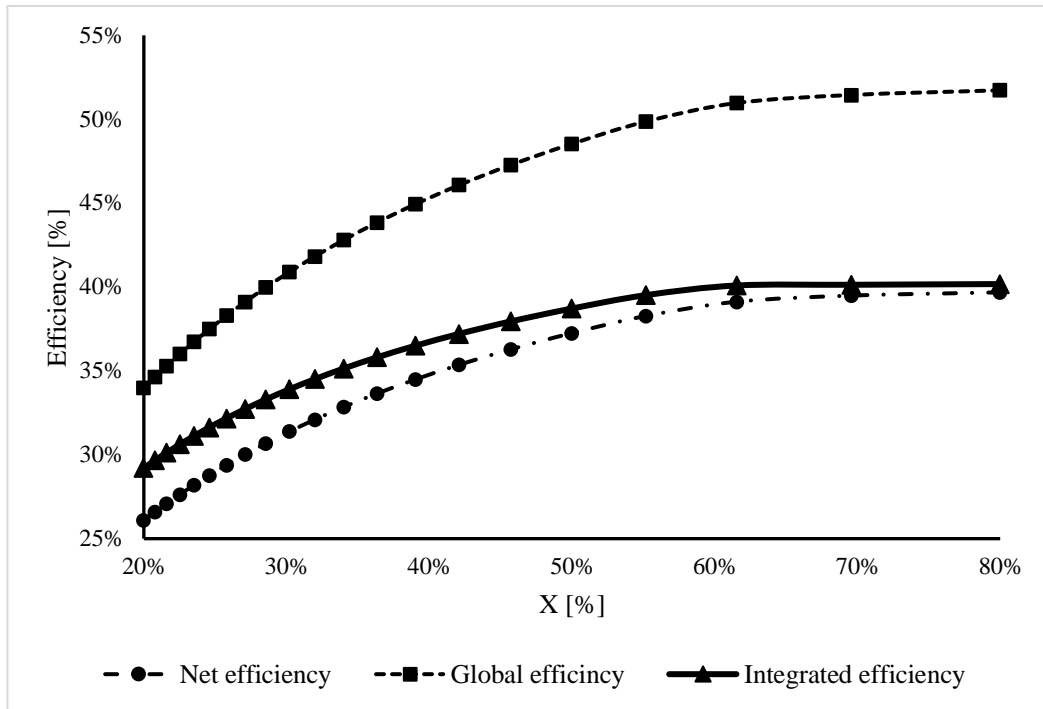
610 *ii. Net efficiency*

$$611 \quad \eta_{NE} = \frac{L_{Rankine} + L_{CO_2, expansion}}{Q_{CSP} + L_{CO_2, compression}} \quad (\text{Eq.}) \quad 23$$

612 *iii. Global efficiency*

$$613 \quad \eta_{GE} = \frac{L_{Rankine} + L_{CO_2, expansion} + Q_{district cooling} + Q_{district heating}}{Q_{CSP} + L_{CO_2, compression} + L_{pump}} \quad (\text{Eq.}) \quad 24$$

614 Figure 19 reports: (i) The integrated efficiency (solid line) defined as energy produced by  
 615 Rankine over input energy from CSP; (ii) the net efficiency (dot-dash line) defined as the ratio  
 616 of energy produced by Rankine and CO<sub>2</sub> work expansion over the heat gathered by the CSP and  
 617 work required during CO<sub>2</sub> compression; (iii) the global efficiency (dot line) defined as the ratio  
 618 of energy produced by Rankine plus CO<sub>2</sub> work expansion and energy heat and cool of secondary  
 619 systems over the heat gathered by the CSP and work required during CO<sub>2</sub> compression.



620

621 **Figure 19: Efficiencies of the TC/CG–ES integrated with Rankine power cycle. Both efficiencies are strongly**  
 622 **dependent of CaO conversion.**

623 Therefore, when the conversion degree X of the sorbent decreases, the material should be  
 624 changed with fresh material in order to increase the efficiency of the system. At high conversion  
 625 levels, the system efficiency increases, reaching almost 40% of integrated and net efficiency,  
 626 exceeding 50% if we supply a district heating and cooling networks consider into global  
 627 efficiency.

628 All the electrical and thermal power streams produced and consumed by the various components,  
 629 and the values of the plant efficiencies at a fixed CaO conversion value set at 0.7 are summarized  
 630 in **Table 5**.

631

**Table 5: Main results obtained at a fixed CaO conversion value set at 0.7**

|                      |                                       |        |
|----------------------|---------------------------------------|--------|
| <b>Calciner side</b> | Power Heat from CSP to calciner [MW]  | -2432  |
|                      | Daylight hours [h]                    | 8      |
|                      | Energy heat from CSP [MWh]            | -19459 |
|                      | Electric power to compress CO2 [MW]   | -208   |
|                      | Electric energy to compress CO2 [MWh] | -1665  |
|                      | Power pump to water networking [MW]   | -1,3   |
|                      | Energy to pump water networking [MWh] | -10    |

|                                  |                                                       |                                |
|----------------------------------|-------------------------------------------------------|--------------------------------|
|                                  | Power to district heating [MW]                        | 232                            |
|                                  | Energy to district heating [MWh]                      | 1856                           |
| <b>Carbonator side</b>           | Electric power from compressed CO <sub>2</sub> [MW]   | 24                             |
|                                  | Electric energy from compressed CO <sub>2</sub> [MWh] | 569                            |
|                                  | Cool power [MW]                                       | 29                             |
|                                  | Cool energy [MWh]                                     | 689                            |
|                                  | Power to Rankine cycle [MW]                           | 745                            |
|                                  | Energy to Rankine cycle [MWh]                         | 17877                          |
|                                  | <b>Rankine cycle</b>                                  | HP T1 [MW]                     |
| HP T2 [MW]                       |                                                       | 39                             |
| MP T1 [MW]                       |                                                       | 54                             |
| MP T2 [MW]                       |                                                       | 43                             |
| LP T1 [MW]                       |                                                       | 43                             |
| LP T2 [MW]                       |                                                       | 38                             |
| LP T3 [MW]                       |                                                       | 23                             |
| LP T4 [MW]                       |                                                       | 35                             |
| P1 [MW]                          |                                                       | -0,1                           |
| P2 [MW]                          |                                                       | -6                             |
| Power output from Rankine [MW]   |                                                       | 326                            |
| Daily work [h]                   |                                                       | 24                             |
| Energy output from Rankine [MWh] |                                                       | 7818                           |
| <b>Efficiency</b>                |                                                       | Thermal Storage efficiency [%] |
|                                  | Storage efficiency [%]                                | 86.8                           |
|                                  | Storage and Recovery efficiency [%]                   | 98.8                           |
|                                  | Rankine efficiency [%]                                | 43.7                           |
|                                  | Integrated efficiency [%]                             | 40.1                           |
|                                  | Net efficiency [%]                                    | 39.5                           |
|                                  | Global efficiency [%]                                 | 51.5                           |

632

#### 633 **4.4 Conclusions**

634 A novel solution for solar energy storage by means of a hybrid thermo-chemical/compressed-gas  
635 energy storage (TC/CG-ES) is presented in this manuscript. The solar energy is used to  
636 decompose CaCO<sub>3</sub> into CaO and CO<sub>2</sub> at high temperature. The produced streams are stored at  
637 ambient temperature. Solar energy is harvested directly into an innovative solar receiver (solid  
638 particles fluidised bed) in which solar radiation collection and energy storage (calcination  
639 reaction) occur simultaneously. The solar energy is stored in chemical form which can be used  
640 in a different place and in a different time without heat loss overcoming the fluctuation of power

641 generation from solar energy. During energy release, CO<sub>2</sub> is expanded into a turbine and sent  
642 into a carbonator where it reacts with CaO coming from silos, and releasing reaction heat at high  
643 temperature, used for power production.

644 An integration with a conventional Rankine cycle rated 320 MWe is proposed. A pinch analysis  
645 is performed to optimize these energy systems. A parametric analysis was carried out to evaluate  
646 the reduction of plant efficiency when varying the main CaL process parameters (such as  
647 carbonation extent, temperature and pressure of carbonation reactor).

648 With respect to molten salt based energy storage the CaL technology has these advantages: (i)  
649 no heat loss (can be used as seasonal storage) while molten salts are sensible storage and therefore  
650 there are thermal loss; (ii) storage temperature equal to environmental temperature (no issue of  
651 solidification) while storage temperature of molten salts have to be higher than solidification  
652 temperature; (iii) maximum temperature achievable very high ( $T_{\text{Carb}}=830^{\circ}\text{C}$ ) while maximum  
653 temperature of molten salts frequently used is  $550^{\circ}\text{C}$ ; (iv) high energy density ( $3.2 \text{ GJ/m}^3$ ) while  
654 energy density of molten salt is  $0.9 \text{ GJ/m}^3$ .

655 The use of CaL process with a conventional Rankine cycle makes this solution a good candidate  
656 for the decarbonisation of the power sector reaching the higher values of Integrated efficiency,  
657 Net efficiency (electric) and Gross efficiency (electric and thermal) equal to 40.1%, 39.5% and  
658 51.5% respectively reaching the higher value of gross efficiency equal to 51.5% providing energy  
659 to district heating and cooling network. The design of the heat exchanger network by means of a  
660 pinch analysis and a parametric study focused on the efficiency of the system when changing the  
661 main KPI (i.e. conversion CaO) were also performed.

662

**Acronyms**


---

|        |                                                       |
|--------|-------------------------------------------------------|
| CaL    | Calcium Looping                                       |
| CSP    | Concentrated Solar Plant                              |
| ECO    | Economizer                                            |
| EVA    | Evaporator                                            |
| GHG    | Green House Gas                                       |
| HEN    | Heat Exchange Network                                 |
| HTF    | Heat Transfer Fluid                                   |
| KPI    | Key Performance Indicator                             |
| PCM    | Phase Change Material                                 |
| RE     | Recovery expander                                     |
| RH     | Re-heater                                             |
| SC     | Storing Compressor                                    |
| SH     | Superheater                                           |
| TCES   | Thermochemical energy storage                         |
| STES   | Sensible thermal Energy Storage                       |
| UNFCCC | United Nations Framework Convention on Climate Change |

**Parameters**


---

|                     |                        |
|---------------------|------------------------|
| $\dot{n}$ [mol/s]   | Molar flow rate        |
| $c_p$ [(J kg)/K]    | Specific heat capacity |
| $G$ [kg/s]          | Mass flow rate         |
| $h$ [kJ/mol]        | Enthalpy               |
| $L$ [MJ]            | Work                   |
| $m$ [kg]            | mass                   |
| $P$ [bar]           | Pressure               |
| $Q$ [MJ]            | Heat                   |
| $T$ [°C]            | Temperature            |
| $t$ [s]             | Time                   |
| $W$ [MW]            | Power                  |
| $X$ [-]             | CaO Conversion         |
| $\Delta H$ [kJ/mol] | Enthalpy difference    |
| $\Delta T$ [°C]     | Temperature difference |

|                            |                            |     |
|----------------------------|----------------------------|-----|
| $\varepsilon$ [-]          | Extent of reaction         | 664 |
| $\eta$ [-]                 | Efficiency                 |     |
| $\Phi$ [MW <sub>th</sub> ] | Thermal power              |     |
| $\nu$ [mol/s]              | Stoichiometric coefficient |     |

### Subscripts

---

|       |                                 |
|-------|---------------------------------|
| c     | cold                            |
| calc  | calciner                        |
| carb  | carbonator                      |
| GE    | Global efficiency               |
| h     | hot                             |
| HP    | High pressure turbine           |
| in    | inlet                           |
| is    | isentropic                      |
| LP    | Low pressure                    |
| min   | minimum                         |
| MP    | Average pressure                |
| NE    | Net efficiency                  |
| out   | outlet                          |
| R     | reaction                        |
| react | reaction                        |
| ref   | reference                       |
| reg   | Regeneration system             |
| SE    | Storage efficiency              |
| SRE   | Storage and recovery efficiency |

- [1] United Nation, «Adoption of the Paris Agreement,» in *Framework Convention on Climate Change*, Paris, 2015.
- [2] International Energy Agency, «Electricity information: Overview,» OECD/IEA, 2018.
- [3] International Energy Agency, «Market Report Series: Renewables 2018. Analysis and Forecast to 2023,» OECD/IEA, 2018.
- [4] T. Schmidla e I. Stadler, «Prospective integration of renewable energies with high capacities using combined heat and power plants (CHP) with thermal storage,» *Elsevier*, 2016.
- [5] International Energy Agency, «Status of power system transformation,» 2018.
- [6] N. Braidenbach, C. Martin, T. Bauer e H. Jockenhofer, «Thermal energy storage in molten salts: Overview of novel concepts and the DLR test facility TESIS,» *Elsevier*, 2016.
- [7] N. P. Siegel, «Thermal energy storage for solar power production,» *John Wiley & Sons, Ltd.*, 2012.
- [8] P. Pardo, A. Deydier, Z. Monvielle e S. Rougé, «A review on high temperature thermochemical heat energy storage,» *HAL*, 2016.
- [9] ENEA, «Solar thermal energy production,» 2001.
- [10] K. Kyaw, H. Matsuda e H. M., «Applicability of carbonation/decarbonation reactions to high-temperature thermal energy storage and temperature upgrading.,» *J Chem Eng Jpn*, vol. 29, p. 119–125., 1996.
- [11] C. Tregambi, F. Montagnaro, P. Salatino e R. Solimene, «A model for integrated calcium looping for CO<sub>2</sub> capture and concentrated solar power,» *Elsevier*, 2015.
- [12] A. Alovio, R. Chacartegui, C. Ortiz, J. M. Valverde e V. Verda, «Optimizing the CSP-Calcium Looping integration for thermochemical energy storage,» *Elsevier*, 2016.
- [13] C. Ortiz, R. Chacartegui, J. M. Valverde, A. Alovio e J. A. Becerra, «Power cycle integration in concentrated solar power plants with energy storage based on calcium looping,» *Elsevier*, 2017.
- [14] R. Chacartegui, A. Alovio, C. Ortiz, J. M. Valverde, V. Verda e J. A. Becerra, «Thermochemical energy storage of concentrated solar power by integration of the calcium looping process and a CO<sub>2</sub> power cycle,» *Elsevier*, 2016.
- [15] T. Shimizu, «A twin fluid-bed reactor for removal of CO<sub>2</sub> from combustion processes,» *ICChem*, 1999.
- [16] S. Stendardo e P. Foscolo, «Carbon dioxide capture with dolomite: A model for gas-solid reaction within the grains of a particulate sorbent,» *Elsevier*, 2009.
- [17] J. M. Valverde, «Ca-based synthetic material with enhanced CO<sub>2</sub> capture efficiency,» *Journal of materials chemistry*, vol. 1, n. 3, 2013.
- [18] H. Chen, C. Zhao, Y. Yang e P. Zhang, «CO<sub>2</sub> capture and attrition performance of CaO pellets with aluminate cement,» *Elsevier*, 2011.
- [19] M. Fujiwara, T. Sano, K. Suzuki e S. Watanabe, «Thermal analysis and fundamental tests on a heat pipe receiver for a solar dynamic space power system,» *Journal of Solar Energy Engineering*, 1990.

- [20] M. M. Kenisarin, «High-temperature phase change materials for thermal energy storage,» *Elsevier*, 2009.
- [21] B. C. Shin, S. D. Kim e W.-H. Park, «Ternary carbonate eutectic (lithium, sodium and potassium carbonates) for latent heat storage medium,» *Solar energy materials*, 1990.
- [22] B. R. Stanmore e P. Gilot, «Review - calcination and carbonation of limestone during thermal cycling for CO<sub>2</sub> sequestration,» *Elsevier*, 2005.
- [23] R. Chirone, P. Salatino, P. Ammendola, R. Solimene e M. Magaldi, «Development of a novel concept of solar receiver/thermal energy storage system based on compartmented dense gas fluidized beds,» in *the 14th international conference on fluidization - From fundamentals to product*, Noordwijkerhout, The Netherlands, 2013.
- [24] N. P. Siegel e I. Ermanoski, «A beam-down central receiver for solar thermochemical hydrogen production,» in *42nd ASES National Solar Conference 2013, SOLAR 2013, Including 42nd ASES Annual Conference and 38th National Passive Solar Conference*, Baltimore, United States, 2013.
- [25] K. Matsubura, Y. Kazuma, A. Sakurai, S. Suzuki e T. Kodama, «High-temperature Fluidized Receiver for Concentrated Solar Radiation by a Beam-down Reflector System,» *Elsevier*, 2013.
- [26] A. Segal e M. Epstein, «COMPARATIVE PERFORMANCES OF `TOWER-TOP' AND `TOWER-REFLECTOR' CENTRAL SOLAR RECEIVERS,» *Elsevier*, 1999.
- [27] A. Poggio, G. Serrati, L. Filippi, C. Maga, L. Manzone e P. Benedetti, «Study on district heating network in the province of Turin: state of the art and potetial development (in italian),» 2006.
- [28] a2a, «Power plant of Monfalcone. Environmental statement 2010. Updating: 31/12/2011 (in italian),» 2011.
- [29] V. Verda e E. Guelpa, *Thermodynamic methods for the efficient use of the energy resources (in italian)*, Esculapio, 2015.
- [30] C. Ortiz, R. Chacartegui, J. M. Valverde, A. Alovio e J. A. Becerra, «Power cycles integration in concentrated solar power plants with energy storage based on calcium looping,» *Elsevier*, 2017.

667

668

669

670 **LIST OF TABLES**

671 **Table 1: Main process parameters of the Rankine power cycle [28]** \_\_\_\_\_ 20  
 672 **Table 2: Streams identified during the pinch analysis of the calciner side** \_\_\_\_\_ 22  
 673 **Table 3: Streams identified during the pinch analysis of the carbonator side** \_\_\_\_\_ 25  
 674 **Table 4: Main operating data of the Calcium Looping storage system** \_\_\_\_\_ 29  
 675 **Table 5: Main results obtained at a fixed CaO conversion value set at 0.7** \_\_\_\_\_ 36  
 676

677 **LIST OF FIGURES**

678 **Figure 1: The Calcium Looping process used as thermochemical storage system. Calcium**  
 679 **oxide and carbon dioxide react together into the carbonator reactor releasing heat of**  
 680 **reaction at high temperature when energy is necessary. The spent material (CaCO<sub>3</sub>)**  
 681 **and unreacted CaO are, at the first time, stored into a silo. These materials are**  
 682 **transported to the calciner to store excess of energy at high temperature with the**  
 683 **inverse reaction.** \_\_\_\_\_ 7  
 684 **Figure 2: Decomposition pressure of Carbon dioxide over calcium carbonate at different**  
 685 **operating temperature [22]** \_\_\_\_\_ 9  
 686 **Figure 3: Integrated Solar Calcium Looping IS-CaL with indirect calcination reaction.**  
 687 **Solar energy is concentrated into a solar receiver up to the tower. The HTF used into**  
 688 **this system is the CO<sub>2</sub> which has the task to provide the heat necessary for the**  
 689 **regeneration of the spent sorbent and to fluidize the calciner.** \_\_\_\_\_ 10  
 690 **Figure 4: Integrated Solar Calcium Looping IS-CaL with direct calcination reaction into**  
 691 **solar calciner. Solar calciner is a solid particles fluidised bed reactor with CO<sub>2</sub> to**  
 692 **separate easily the product of calcination reaction. The compounds are stored at**  
 693 **ambient temperature to avoid thermal losses.** \_\_\_\_\_ 11  
 694 **Figure 5: Thermo-Chemical/Compressed-Gas Energy Storage (TC/CG-ES) coupled with**  
 695 **a conventional Rankine power cycle. During sunlight solar energy can be transformed**  
 696 **directly in electricity or stored in chemical compound. There are three operational**  
 697 **phase: (i) Only electricity is produced; (ii) only charging of storage system; (iii) Both**  
 698 **electricity and chemical compounds are produced.** \_\_\_\_\_ 14  
 699 **Figure 6: Train of five compressors with five inter-coolers. The heat at low temperature**  
 700 **provided during compression, supply a district heating network.** \_\_\_\_\_ 15  
 701 **Figure 7: District cooling network used to avoid the condensation of the CO<sub>2</sub> and associate**  
 702 **danger for the blade of turbine. The water used into the inter-heating at 12°C, is cooled**  
 703 **until 6°C.** \_\_\_\_\_ 15  
 704 **Figure 8: Molar balance schematic of the Calcium Looping process. In the right side**  
 705 **calcination reaction and energy storage happen; In the other side CaO and CO<sub>2</sub> react**  
 706 **into carbonator reactor and the heat of reaction is transported by the CO<sub>2</sub> used as**  
 707 **HTF.** \_\_\_\_\_ 16  
 708 **Figure 9: Energy balance of the storage system focused on the main critical reactors.** \_\_\_\_ 19  
 709 **Figure 10: Release of energy via TC/CG-ES integrated with Rankine power cycle. The**  
 710 **CO<sub>2,recycle</sub> fluidises the carbonator reactor and transfer heat to Rankine cycle.** \_\_\_\_ 21  
 711 **Figure 11: Composite curve of the solar calciner side. Section A represents the excess of**  
 712 **heat at low temperature; in section B the hot streams provide heat to cold streams; in**

|     |                                                                                                         |    |
|-----|---------------------------------------------------------------------------------------------------------|----|
| 713 | section C there aren't hot streams and the heat enough is provided by CSP to cold                       |    |
| 714 | streams                                                                                                 | 23 |
| 715 | <b>Figure 12: a) Minimum energy consumption network inferred from the pinch analysis in</b>             |    |
| 716 | <b>the calciner side. The values of temperature level are reported in degree Celsius. b)</b>            |    |
| 717 | <b>Plant configuration (calciner-side) resulting from the pinch analysis</b>                            | 24 |
| 718 | <b>Figure 13: Composite curve of the carbonator side. Section A represents the excess of heat</b>       |    |
| 719 | <b>at low temperature; in section B the hot streams provide heat to cold streams; in</b>                |    |
| 720 | <b>section C there aren't hot streams and the heat enough is provided by carbonation</b>                |    |
| 721 | <b>reaction to cold streams</b>                                                                         | 26 |
| 722 | <b>Figure 14: a) Minimum energy consumption network inferred from the pinch analysis in</b>             |    |
| 723 | <b>the calciner side. The values of temperature level are reported in degree Celsius. b)</b>            |    |
| 724 | <b>Plant configuration (carbonator-side) resulting from the pinch analysis.</b>                         | 27 |
| 725 | <b>Figure 15: a) Thermal power fluxes of main reactors at varying CaO conversion. b) The</b>            |    |
| 726 | <b>heat enough from Rankine cycle is fixed, while change the heat provides by the storage</b>           |    |
| 727 | <b>system.</b>                                                                                          | 31 |
| 728 | <b>Figure 16: Parametric analysis: Daily storage volume with the change of CaO conversion</b>           |    |
| 729 |                                                                                                         | 32 |
| 730 | <b>Figure 17: Trend of two KPI (Thermal Storage efficiency and Storage efficiency) function</b>         |    |
| 731 | <b>of carbonator pressure.</b>                                                                          | 34 |
| 732 | <b>Figure 18: It is illustrated with whole line the thermal energy (left axis) of the heat provided</b> |    |
| 733 | <b>by carbonator reactor (square indicator) and heat input to CSP power plant (triangle</b>             |    |
| 734 | <b>indicator). With the dash line is represented the three different efficiency of the storage</b>      |    |
| 735 | <b>system (right axis). These parameters are function of CaO conversion.</b>                            | 34 |
| 736 | <b>Figure 19: Efficiencies of the TC/CG–ES integrated with Rankine power cycle. Both</b>                |    |
| 737 | <b>efficiencies are strongly dependent of CaO conversion.</b>                                           | 36 |
| 738 |                                                                                                         |    |